AECL-6835

ATOMIC ENERGY OF CANADA LIMITED

L'ENERGIE ATOMIQUE DU CANADA, LIMITEE

SAFETY RESEARCH FOR CANDU REACTORS

RECHERCHES SUR LA SECURITE DES REACTEURS CANDU

W. T. Hancox

A paper presented to the International Atomic Energy Technical Committee Meeting on Thermal Reactor Safety Research in Moscow, 1981 December 1-4.

Communication présentée à la Réunion du comité technique de l'Agence internationale de l'énergie atomique sur les recherches sur la sécurité des réacteurs thermiques, Moscou, 1-4 décembre 1981.

Whiteshell Nuclear Research Establishment

Etablissement de recherches nucléaires de Whiteshell

Pinawa, Manitoba R0E 1L0

October 1982 octobre

ATOMIC ENERGY OF CANADA LIMITED

SAFETY RESEARCH FOR CANDU REACTORS

by

W.T. Hancox

A paper presented to the International Atomic Energy Agency Technical Committee Meeting on Thermal Reactor Safety Research in Moscow, 1981 December 1-4.

Whiteshell Nuclear Research Establishment
Pinawa, Manitoba ROE 1LO
1982 October

AECL-6835

RECHERCHES SUR LA SECURITE DES REACTEURS CANDU*

par

W.T. Hancox

RESUME

Ce rapport décrit les recherches en cours pour développer et vérifier les modèles informatiques pour les systèmes de sécurité et du procédé des réacteurs CANDU-PHW**. Il porte surtout sur les accidents de perte de caloporteur (LOCA) parce que ceux-ci sont les précurseurs d'accidents plus graves. Les sujets de recherche, qui sont influencés par les caractéristiques intrinsèques relatives à la sécurité qui distinguent les réacteurs CANDU-PHW des autres réacteurs thermiques refroidis à l'eau, comprennent:

(i) les processus de transfert de chaleur et la dynamique des fluides dans le système de caloportage au cours des phases de vidange et de remplissage des LOCA;

(ii) le comportement mécanique et le comportement thermique des éléments de combustible;

(iii) le comportement mécanique et le comportement thermique du combustible et des ensembles de canaux de combustible dans des situations dans lesquelles le modérateur à l'eau lourde absorbe la chaleur résiduelle produite dans le combustible;

(iv) le comportement chimique des gaz de fission qui pourraient être rejetés dans le caloporteur du réacteur et transportés au système de confinement;

(v) la combustion des mélanges hydrogène-air-vapeur qui seraient produit si les températures du combustible étaient assez élevées pour provoquer une réaction zirconium-eau.

On fait ressortir les points saillants de l'état présent des recherches sur chacun de ces sujets en insistant particulièrement sur les conclusions auxquelles on a abouti à date et leur impact sur le programme en cours.

* Communication présentée à la Réunion du comité technique de l'Agence internationale de l'énergie atomique sur les recherches sur la sécurité des réacteurs thermiques, Moscou, 1-4 décembre 1981.

** CANada Deuterium Uranium - Pressurized Heavy Water/Canada Deuterium Uranium - Eau lourde sous pression

L'Energie Atomique du Canada, Limitée
Etablissement de recherches nucléaires de Whiteshell
Pinawa, Manitoba ROE 1LO
1982 octobre

AECL-6835

SAFETY RESEARCH FOR CANDU REACTORS*

by

W.T. Hancox

ABSTRACT

Continuing research to develop and verify computer models of CANDU-PHW** reactor process and safety systems is described. It is focussed on loss-of-coolant accidents (LOCAs) because they are the precursors to more serious accidents. The research topics are influenced by intrinsic safety-related characteristics that distinguish CANDU-PHW reactors from other water-cooled thermal reactors and include:

(i) fluid-dynamic and heat-transfer processes in the heat-transport system during the blowdown and refilling phases of LOCAs;

(ii) thermal and mechanical behaviour of fuel elements;

(iii) thermal and mechanical behaviour of the fuel and the fuel-channel assembly in situations where the heavy-water moderator is the sink for decay heat produced in the fuel;

(iv) chemical behaviour of fission gases that might be released into the reactor coolant and transported to the containment system;

(v) combustion of hydrogen-air-steam mixtures that would be produced if fuel temperatures were sufficiently high to initiate the zirconium-water reaction.

The current status of the research on each of these topics is highlighted with particular emphasis on the conclusions reached to date and their impact on the continuing program.

* Paper presented at the International Atomic Energy Agency Technical Committee Meeting on Thermal Reactor Safety Research, Moscow, 1981 December 1-4.

** CANada Deuterium Uranium - Pressurized Heavy Water.

Atomic Energy of Canada Limited
Whiteshell Nuclear Research Establishment
Pinawa, Manitoba ROE 1LO
1982 October

AECL-6835

CONTENTS

INTRODUCTION

This paper describes continuing research to develop and verify computer models of CANDU-PHW reactor process and safety systems. In common with other water-cooled reactors, loss-of-coolant accidents (LOCAs) in CANDU-PHWs are the precursors to more serious accidents and are the focus of the research.

The choice of research tasks is influenced by intrinsic safety-related characteristics that distinguish CANDU-PHWs from other water-cooled thermal reactors. Figure 1 shows a section through a CANDU-PHW core, the source of one of the unique safety-related features. The core consists of an array of horizontal pressure tubes that pass through a large cylindrical calandria. The pressure tubes contain the fuel bundles and the high pressure, heavy-water coolant. The calandria is filled with cool (about 70°C) heavy-water moderator that is insulated from the hot reactor coolant by a calandria tube around the pressure tube, but separated from it by a gas-filled annulus. The heavy-water moderator is continuously cooled, providing a sink for decay heat produced in the fuel if there is a LOCA and a coincident failure of the emergency coolant injection (ECI) system. Because the fuel is separated from the moderator by only the relatively thin pressure and calandria tubes, it cannot become very hot and remain insulated from the moderator.

The primary heat-transport (PHT) circuit, shown in Figure 2, is arranged in a figure-of-eight, with two pumps and two steam generators. The term figure-of-eight refers to a circuit in which coolant passes through the core to a steam generator and is then pumped back through the core into another steam generator and pump. The fuel channels in each core pass are individually connected by small diameter feeder pipes (50 to 80 mm I.D.) to horizontal headers located above the core at each end. This arrangement minimizes the amount of large diameter piping: 98% of the piping length has a diameter less than 100 mm. This means that the most likely LOCAs will be initiated by small breaks that are relatively easy to cope with. It also means that the transient steam-water flows that evolve during a LOCA are well represented by one-dimensional mathematical models; that is, models in which the steam and water parameters are averaged over the flow cross-section. In addition, important fluid-dynamic and heat-transfer processes associated with LOCAs can be readily studied using full-size components such as fuel channels, feeders and flow distribution headers. These factors simplify the development of calculation methods and the demonstration of calculation accuracy.

The major safety research tasks and their interactions are shown in Figure 3. Included are the mathematical models and the associated experiments required to determine:

(i) fluid-dynamic and heat-transfer processes in the heat-transport system during the blowdown and refilling phases of a LOCA;

(ii) thermal and mechanical behaviour of individual fuel elements;

(iii) thermal and mechanical behaviour of the fuel and the fuel-channel assembly in situations where the heavy-water moderator system is the dominant heat sink;

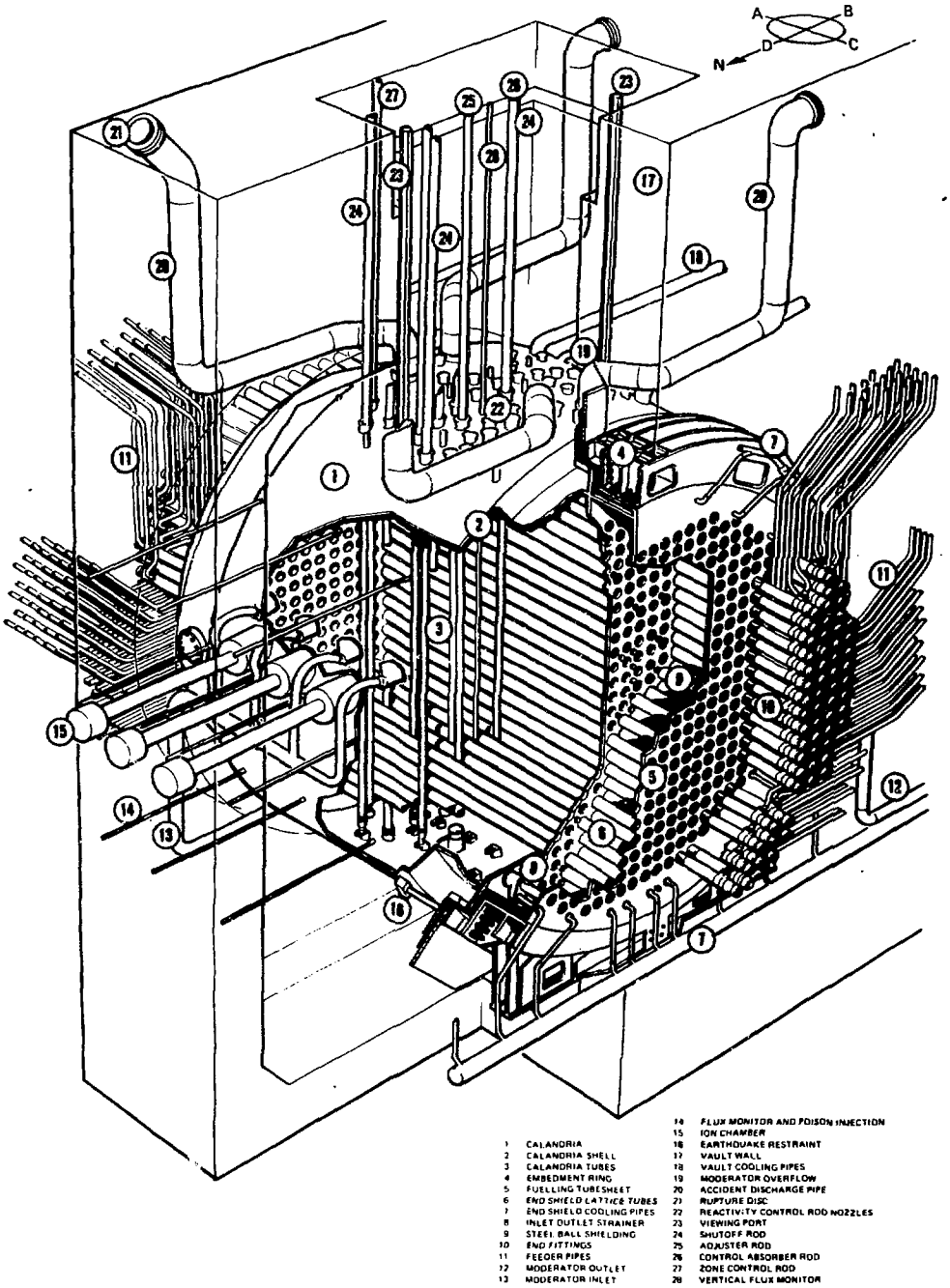

FIGURE 1: Cutaway of a CANDU Reactor Core

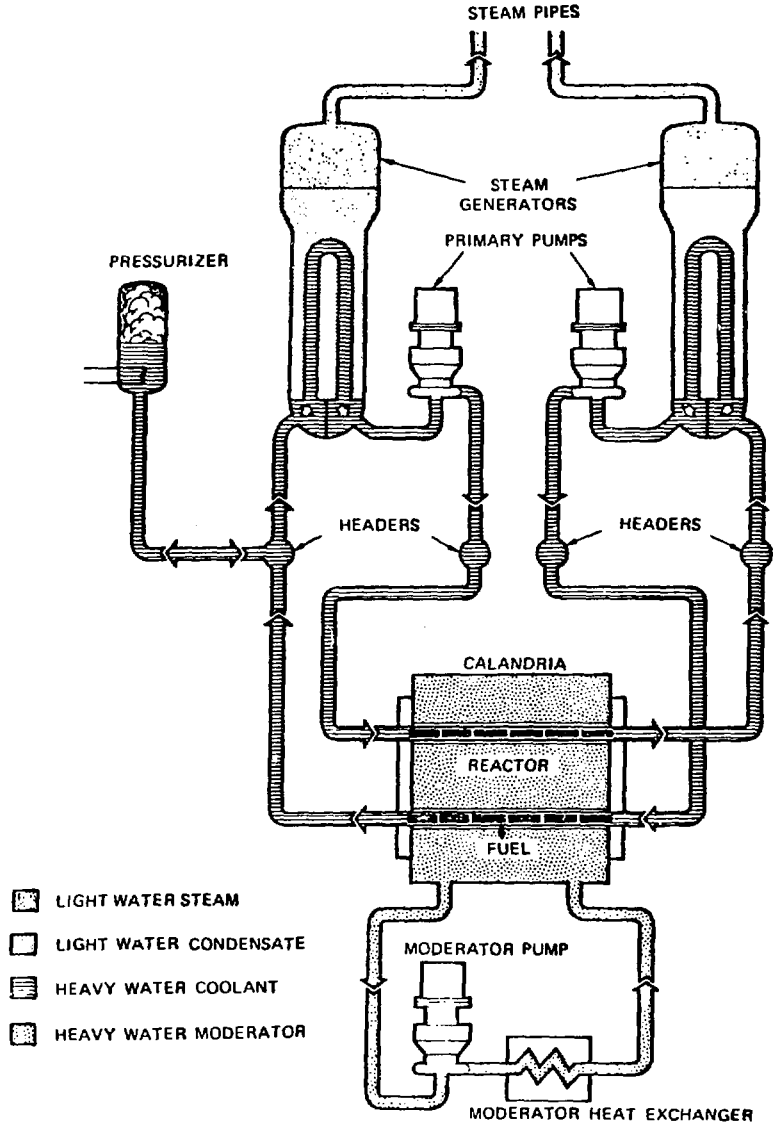

FIGURE 2: Simplified Diagram of a CANDU Reactor Heat-Transport System

(iv) the chemical behaviour of fission gases that might be released into the reactor coolant and transported to the containment system;

(v) the effects of combustion of hydrogen-air-steam mixtures in the containment system if fuel temperatures are sufficiently high to initiate the zirconium-water reaction.

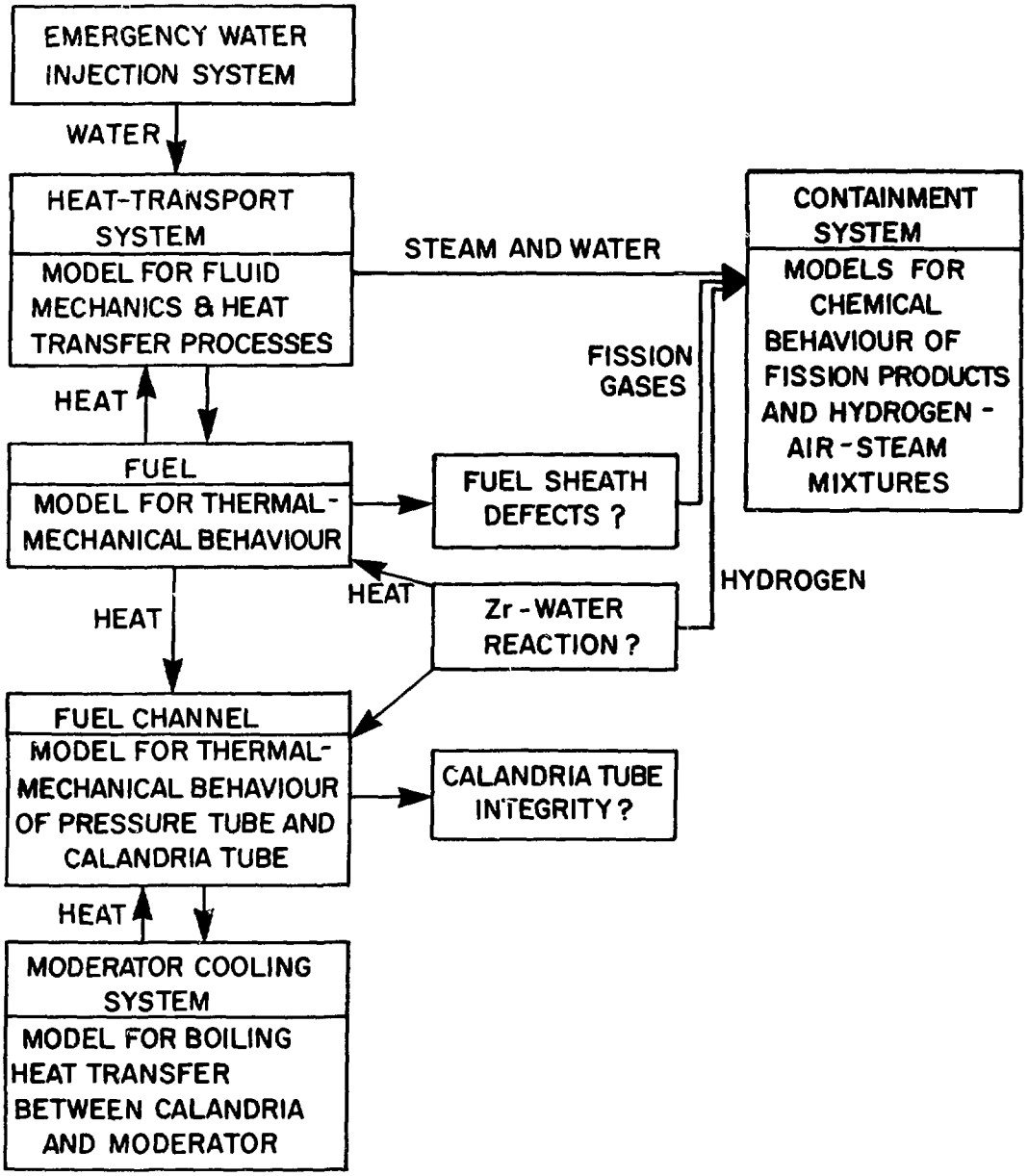

FIGURE 3: LOCA Research Tasks and Their Interactions

Our modelling strategy is illustrated in Figure 4. It involves establishing a sound theoretical basis for the models and then verifying them systematically against experiments. An alternative approach is to start with very large and complex simulation experiments that provide an empirical basis for the calculations. The strategy shown in Figure 4 minimizes the resources required. First, starting from fundamental physical

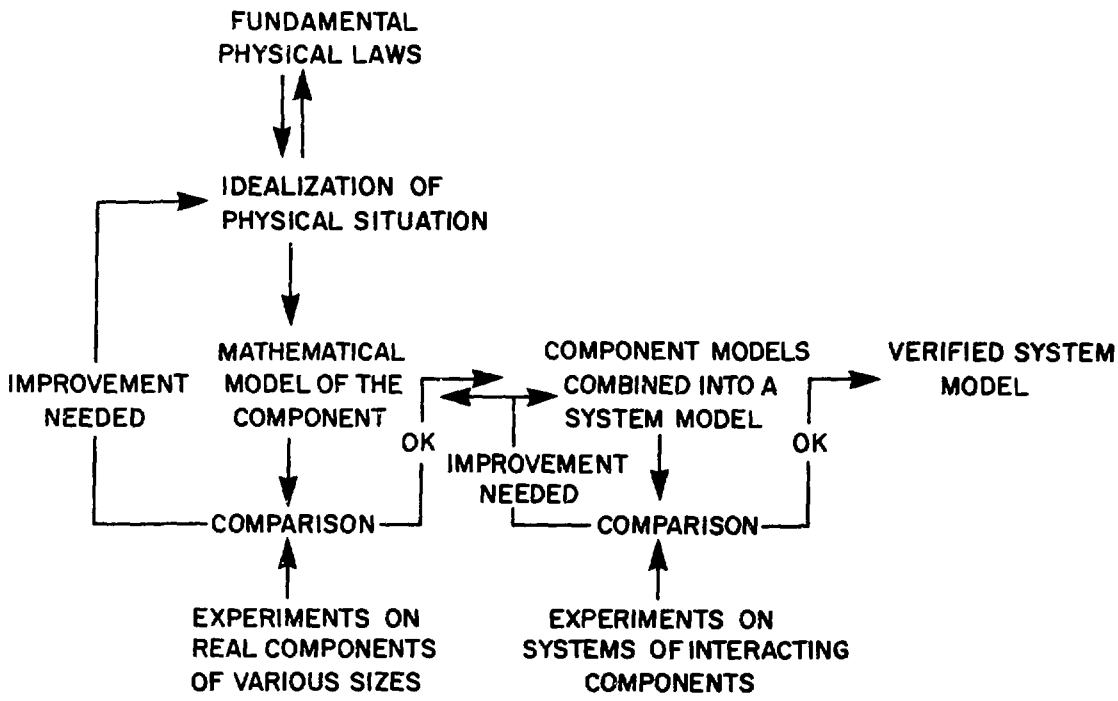

FIGURE 4: Modelling Strategy

principles, models are developed for the important components, and then checked against experiments on real components. As noted above, in many cases experiments can be done on full-size components. Where such experiments are not practical, several geometrically similar, but smaller, components are tested to determine scaling factors. The component models are then assembled into an integrated model of the system, which is checked against experiments on systems that have the essential geometrical and physical characteristics of the reactor system. The product is a computer model of the reactor system that gives predictions of known accuracy.

The current status of the research associated with each of the tasks is summarized below. Particular emphasis is given to the conclusions reached to date and their impact on the continuing program.

THERMALHYDRAULICS

Model Development

Research on improved mathematical models for the heat-transport system started in 1974, leading to the development of the computer code RAMA [1,2]. It is an assembly of mathematical models representing each of the

components in a CANDU-PHW PHT circuit. Figure 5 is a schematic diagram of the circuit arrangement as it is simplified for RAMA calculations. The multiple parallel fuel channels of a reactor core pass are represented by two equivalent fuel channels: one representing the bulk of the fuel channels at the average core power, and one representing the few channels at the peak core power. Individual circuit components (such as the pumps, headers and fuel channels) may be represented by either distributed or lumped-parameter models. In the former, dependent variables are represented as functions of both time and space within the component (partial differential equations), while in the latter, the spatial dependence is eliminated by integration (ordinary differential equations in time). The choice of whether to represent a specific component by a distributed or lumped--parameter model is made according to the level of detail required to reproduce the important physical phenomena.

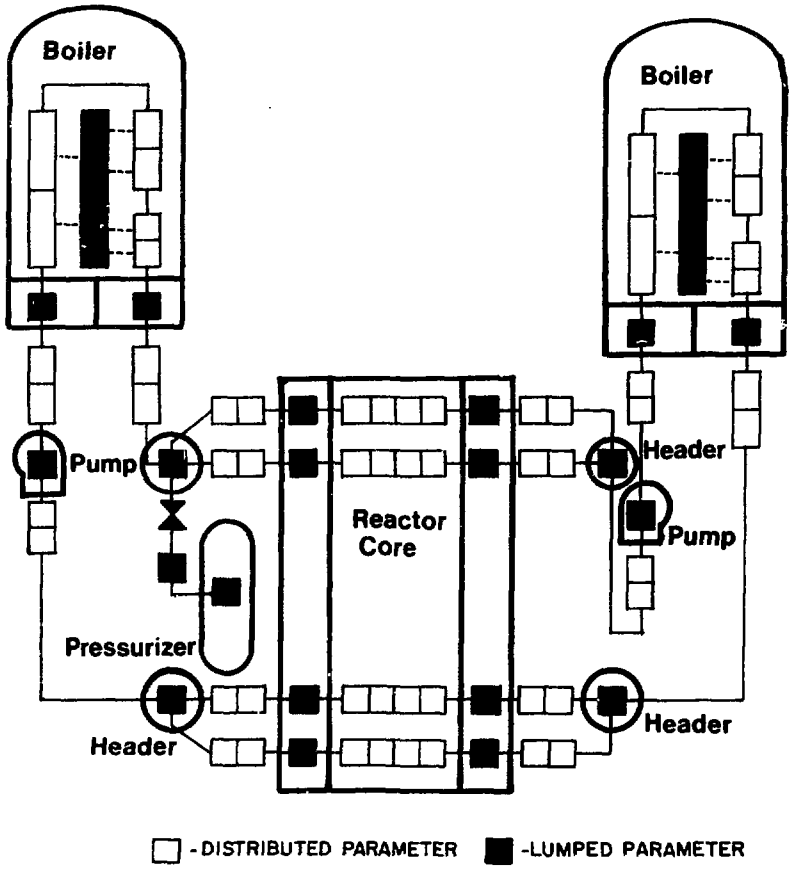

FIGURE 5: Idealization of a CANDU Reactor PHT System for Analysis with the Computer Code RAMA

The PHT system consists basically of a network of relatively small-diameter pipes. As a result, the flow variables may be averaged over the flow cross-section without losing important physical detail. One-dimensional conservation equations are therefore appropriate. A range of models of varying sophistication is possible: the simplest model considers the flow of a homogeneous mixture of steam and water in thermal equilibrium (the steam and water are assumed to have equal velocities and equal temperatures at each point along the flow path, an EVET model); the most sophisticated model assumes that the steam and water flow in separate streams with different velocities and temperatures (an unequal velocity, unequal temperature, or UVUT model) [3-5]. The flow-boiling models currently available in RAMA are listed in Table 1. Of these, the UVUT model is still being developed.

TABLE 1

FLOW-BOILING MODELS

Model Description	No. of Partial Differential Equations	Examples of Dependent Variables	Constitutive Equation	Use
homogeneous equilibrium (EVET)	3	mixture velocity, enthalpy, pressure	heat, momentum transfer between mixture and duct	blowdown
non-equilibrium (EVUT)	5	velocity, void fraction, pressure, phase temperature	heat, momentum transfer to the duct wall, interphase heat transfer	cold water injection
separated flow (UVUT)	6	phase velocities, enthalpies, one pressure, void fraction	wall-to-phase and phase-to-phase mass momentum and energy transfer	stratified and counter-current flow

The partial differential equations comprising the various flow-boiling models all have a common mathematical form; only the number of equations varies from model to model. They are solved using a characteristic finite-difference method [6,7] that is particularly suited to the reactor circuit. A dynamic mesh point allocation technique is used to control the solution accuracy during transients with steep spatial gradients (such as occur when cold water is injected into steam) [7,8]. This makes the mesh dense where gradients are steep, sparse where gradients are shallow, and moves the mesh with the gradient if it propagates.

In addition to the models for flow in the pipe network, models are required for the pumps, headers, and steam-generator secondary sides. Models are also required for thermal behaviour of the fuel and for the reactor kinetics. Table 2 lists the models currently used in RAMA. The steam-generator secondary side can be represented by a lumped-parameter model or, when spatial effects are important, by applying the flow-boiling equations to a discretized representation of the boiler secondary flow loop (downcomer, riser, steam drum). Thermodynamic and transport properties are available in an efficient package, and subroutines are included for heat-transfer coefficients and friction factors as functions of the local steam and water conditions.

TABLE 2

COMPONENT AND AUXILIARY MODELS

Model	To Compute	Description
pump	shaft work	empirical lumped-parameter model
radial heat conduction	heater, fuel or pipe wall temperature	variation solution of radial heat-conduction equation
reactor kinetics	neutron power	6-group point neutronics, 3-group decay heat, with appropriate reactivity feedback and reactor trip logic
boiler secondary side	heat-transfer rate	lumped-parameter model for conservation of mass and energy
break	discharge rate	orifice equation for subcooled discharge, sonic discharge otherwise
in-line orifice or valve	pressure drop	orifice equation for compressible flow
transfer coefficients	heat-transfer coefficient, friction factor, two-phase multiplier	empirical correlations
volume element	holdup in volumes such as headers and boiler plenums	point conservation equations without spatial terms (ordinary differential equations in time)
abrupt area change	pressure drop	steady-state conservation equations with empirical expansion and contraction losses

The theoretical soundness of the flow-boiling models and the numerical solution procedure has been thoroughly checked against benchmark problems and fundamental experiments [9-12].

Experiments

In parallel with the mathematical modelling, an extensive program of experiments is essential. Two types have already been done: experiments to determine the behaviour of components such as fuel channels [13,14], pumps [15,16], steam generators [17], and flow distribution headers with the steam-water flows expected in a LOCA; and experiments on the RD-4 [18] and RD-12 [19-21] loops, with components arranged as they are in a reactor heat-transport system, to determine the response to breaks of various sizes in an inlet or outlet header. These experiments have served two purposes. First, they have provided detailed information on the important physical processes to guide the formulation and check the viability of the mathematical models. Second, they have provided an empirical basis for the design of emergency coolant injection systems.

To study refilling processes, we have done experiments on the facility shown in Figure 6. Each of the two horizontal channels consists of a 6-m

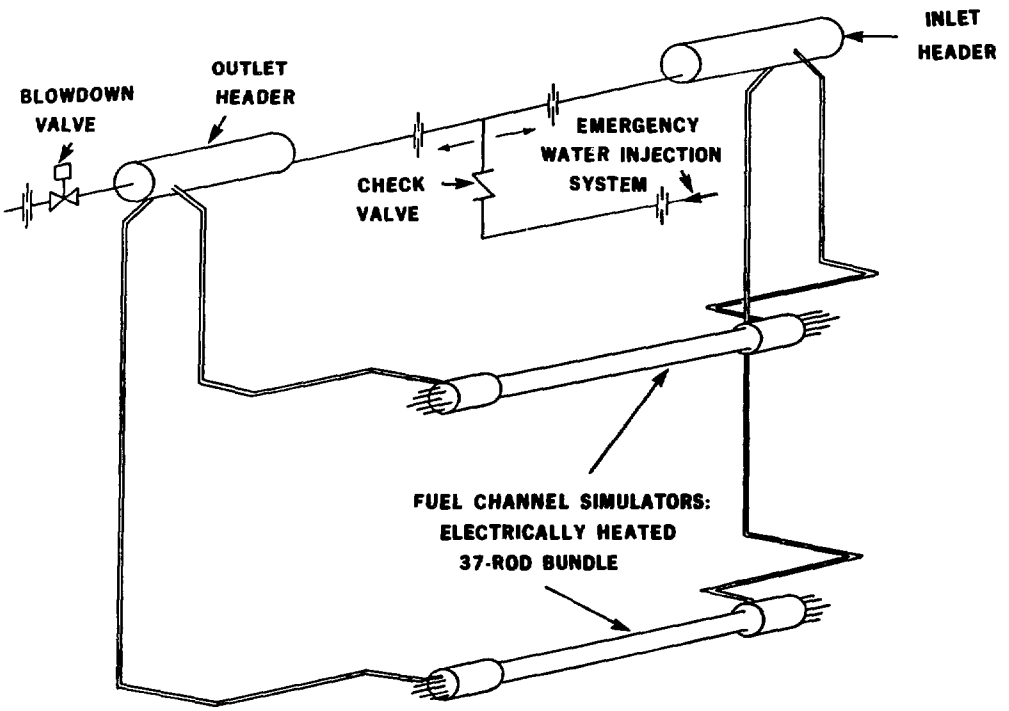

FIGURE 6: Experimental Facility Used to Study Refilling of Hot Steam-Filled Horizontal Fuel Channels

long 100-mm diameter flow tube containing a 6-m long bundle of thirty-seven electrically heated 13-mm diameter rods. The channels, therefore, have the same geometry as typical CANDU fuel channels, excluding the end fittings. They are connected to inlet and outlet headers by 50-mm diameter pipes. A water injection system, consisting of a pump (or an accumulator) controlled to give a constant discharge pressure up to 900 kPa (or 4 MPa), is connected to the inlet header, or both the inlet and outlet headers, through a one-way valve.

The initial conditions for an experiment are established by circulating superheated steam to raise the temperature of the pipes to 300°C, and then isolating the loop with an internal pressure greater than the injection pressure. Next, electrical power is supplied to the rods and, when their surfaces reach the desired temperature (usually 400°C), blowdown of the loop is initiated by opening a gas-actuated valve in the discharge line from the outlet header. Cold water is injected automatically when the loop pressure is less than the injection pressure. The desired channel flow conditions are achieved by an appropriate combination of injection pressure and break size.

Figure 7 summarizes the results of several experiments done with a single channel. It shows the time difference between rewetting of upper and lower rods at the channel outlet as a function of the average refilling rate. At high refilling rates (greater than 1 kg/s), the injected water accelerates rapidly and propagates through the channel like a piston. Upper and lower rods rewet simultaneously. This physical picture is consistent with the EVET model and good agreement between experiment and prediction is achieved. On the other hand, at refilling rates less than 1 kg/s, the flow in the channel stratifies. The rod temperature transients show that the injected water flows in a layer along the bottom of the channel, rewetting the lower rods. Steam generated during rewetting flows out through the upper part of the channel, removing heat from the upper rods and gaining substantial superheat. As the injection proceeds, the water level rises, progressively rewetting more rods until the channel is filled. Thus the flow is initially characterized by high-velocity, superheated steam flowing over an essentially stationary layer of sub-cooled water.

Figure 8 shows typical rod temperature transients measured during an experiment with an average refilling rate of about 0.3 kg/s. Temperature transients calculated by the RAMA code using both the EVET and EVUT models are also shown. As evident, neither the EVET model nor the EVUT model is in good agreement with the measured temperatures. The EVET model assumes that the steam and water are uniformly distributed over the flow cross-section and that they are in thermal equilibrium. This means that the sink temperature for heat transfer is the local saturation temperature. Therefore, lower rods are predicted to have the same temperature as upper rods.

The EVUT model assumes that the steam and water streams have different temperatures but equal velocities. Hence, it removes one of the weaknesses of the EVET model - the assumption of thermal equilibrium - and should yield more accurate predictions. As evident from Figure 8, although there is some improvement in the agreement between prediction and experiment, the EVUT model does not predict the same degree of stratification as is observed in

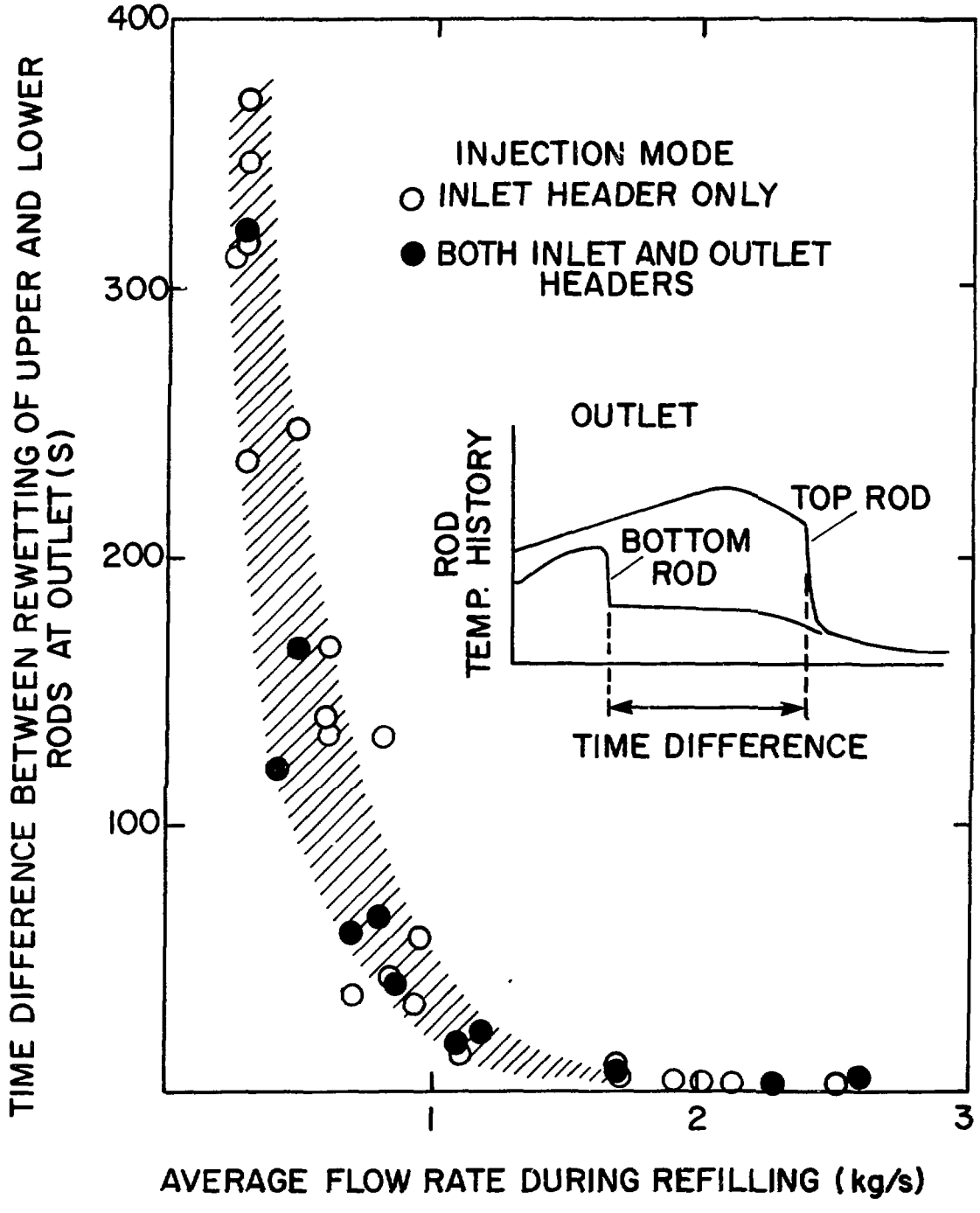

FIGURE 7: Duration of Flow Stratification as a Function of Refilling Rate for Experiments Done with a Single Channel

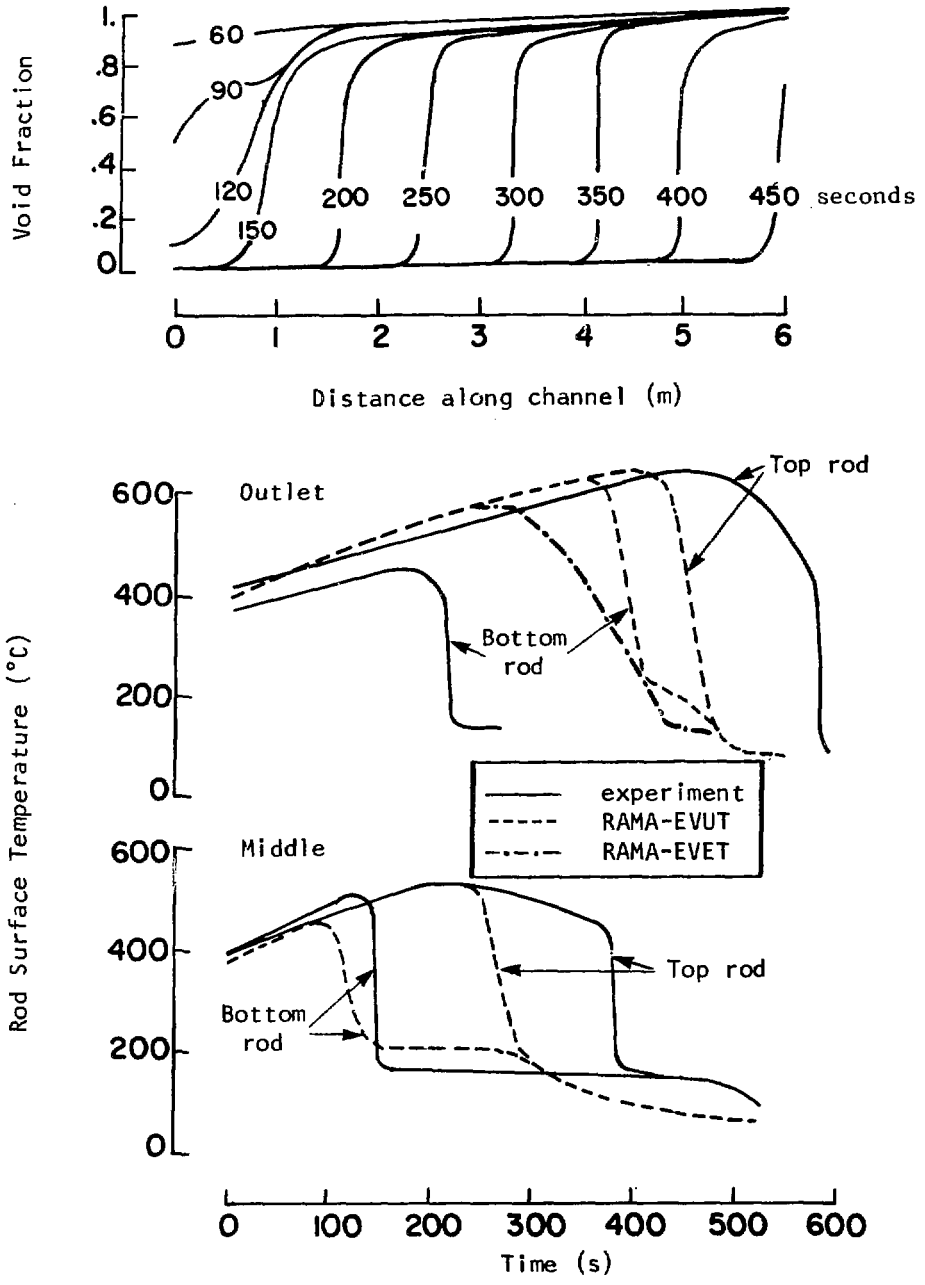

FIGURE 8: Measured and Predicted Rod Temperature Transients for an Experiment Done at Low Refilling Rate

the experiment. This is most clearly shown by the evolution of the channel void profiles at the top of Figure 8. The EVUT model predicts that the flow is initially stratified, but as cooling proceeds the injected water quickly steepens into a vertical front. The effect is, therefore, very similar to that produced by the EVET model; both the maximum temperature and the refilling time are under-predicted.

The above result is typical of that obtained for a range of refilling experiments done with low refilling rates. EVET and EVUT models under-predict both maximum rod temperatures and refilling times, and the size of the error increases as the refilling rate decreases. To improve the prediction accuracy, mathematical models must allow for the flow of steam and water in separate streams with different velocities and temperatures. Models with this capability (called unequal velocity, unequal temperature, or UVUT models) are being developed and are the focus of continuing research.

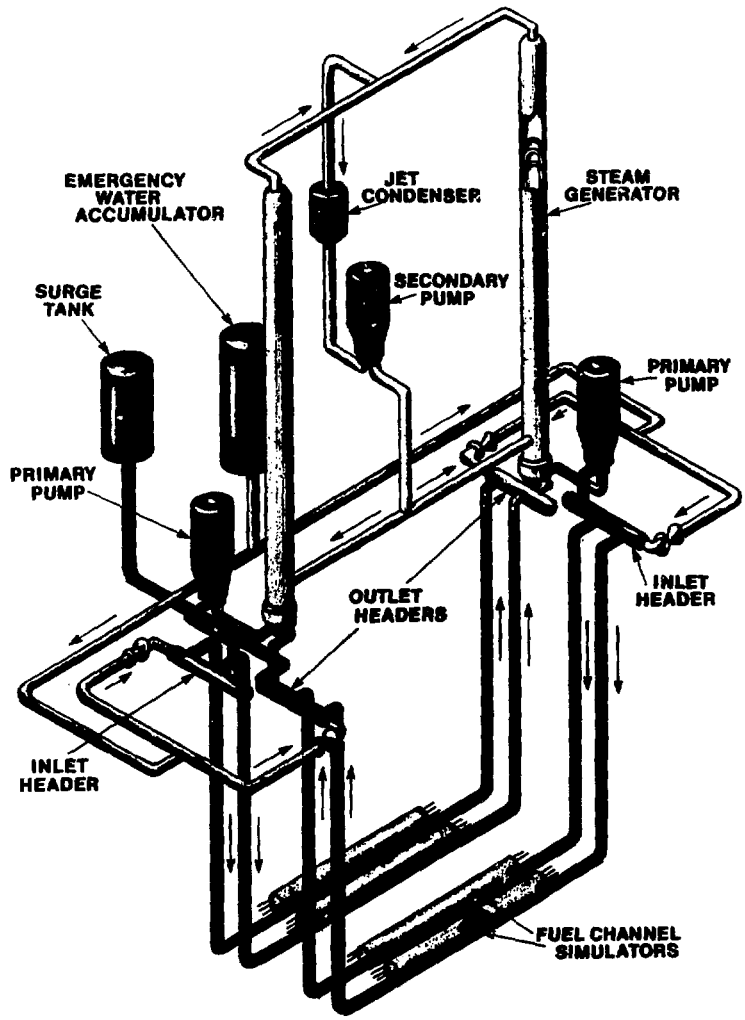

FIGURE 9: Schematic of the Experimental Facilities Used to Study Blowdown and Refilling Processes in the Primary Heat-Transport System

To check the integrated behaviour of the RAMA code, we have done experiments using pressurized, recirculating water loops (RD-4 and RD-12) with the figure-of-eight circuit arrangement shown in Figure 9. Table 3 lists the essential characteristics of these loops as well as the RD-14 loop which is currently being built. The experiments involve blowdown through breaks of various sizes in either an inlet header or an outlet header, followed by water injection from an accumulator. During the resulting transients, measurements are made of the heated rod temperatures and of coolant temperature, pressure, density and flow rate at selected locations around the circuit.

TABLE 3

CHARACTERISTICS OF THE RD-4, RD-12 and RD-14 LOOPS

	RD-4	RD-12	RD-14
Pressure (MPa)	4.5	10	10
Volume (m^3)	0.053	0.34	0.73
Heated Channels	tube	7 rods	37 rods
Length (m)	1.5	4	6
Rod diameter (mm)	13.4	15.2	13.1
Flow-tube diameter (mm)		51.7	103.4
Power (kW)	100	1500	5500
Pumps	------single-stage centrifugal------		
Flow (kg/s)	0.5	6	24
Heat Sink	single-tube heat exchanger	recirculating-tube steam generator	
Elevation Difference (m)	8	9.6	22

The experiments show that there is a wide range of conditions for which the steam and water phases are well mixed throughout most of the transient. In these situations, good agreement is obtained between experiment and predictions of the RAMA code using the EVET model. However, there are a few combinations of break size and location that result in an initial period of flow stagnation in one of the heated sections. These critical or stagnation breaks produce the highest rod temperatures and the longest refill times. Their magnitude depends on the injection pressure and the power input to the heated section during the transient*. The stagnation

* It should be noted that CANDU reactors have a slightly positive void-reactivity coefficient. For the fastest voiding rate, including the effect of loss of one shutdown system, the resulting power pulse is about 2.5 full-power seconds.

breaks are characterized by initially low flow velocities that lead to steam-water separation. This separation occurs first in horizontal portions of the circuit, such as heated sections and headers, when the local pressure gradient is sufficiently small that the inertial forces acting on the flow are overtaken by the gravitational force. The water settles and the flow stratifies. Once separation is established locally, it spreads, affecting the distribution of steam and water throughout the circuit. The steam and water streams interact, but only weakly. The steam is more mobile than the water and acquires a much higher velocity. The weak interaction between the streams also means that they can achieve different temperatures. As might be expected, agreement between experiment and predictions of the RAMA code, using the EVET model, is poor. Again, an UVUT model is required.

Figure 10 shows measured and predicted maximum temperatures for heated rods in the hottest section of the RD-4 and RD-12 loops for inlet header breaks of various sizes and for the initial blowdown phase prior to water injection. For the RD-4 loop, a significant short-term excursion occurs only for a small range of break sizes because friction at the pipe walls is the dominant resistance to flow, owing to the large surface area to volume ratio. As a result, changes in resistance caused by increasing or

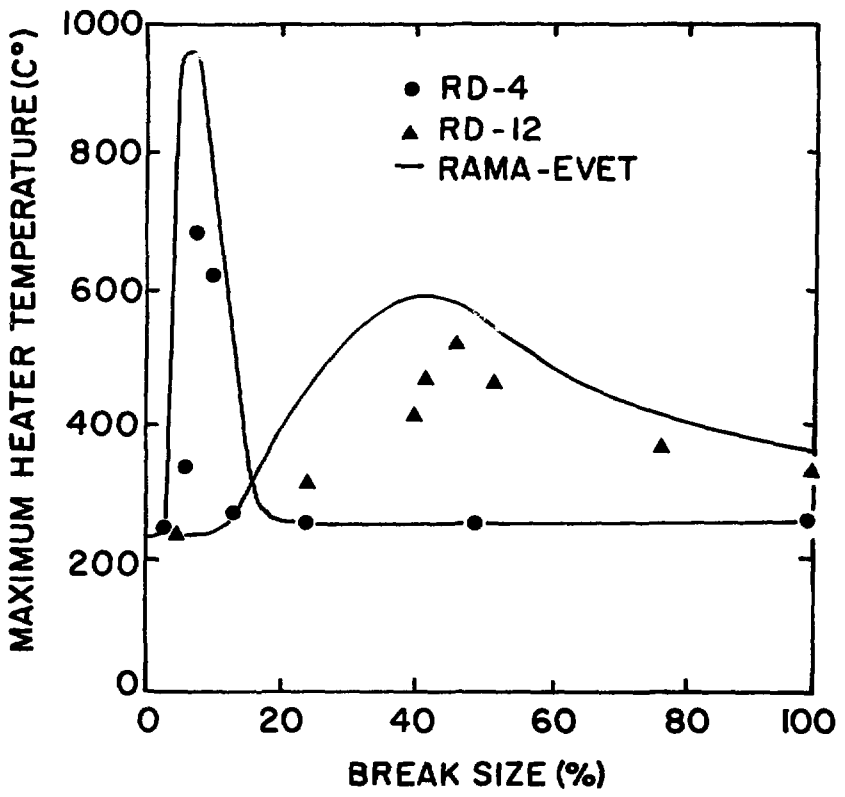

FIGURE 10: Variation of the Initial Peak Temperature with Break Size for Inlet-Header Breaks in the RD-4 and RD-12 Loops

decreasing the break size have little effect. Temperature excursions are observed over a wider range of break sizes in RD-12 because the effect of pipe friction is less important due to its much smaller surface area to volume ratio. As evident, agreement is good between experiment and prediction using the RAMA code with the EVET flow model. RAMA correctly predicts the critical break size but generally over-predicts the maximum temperature. The over-prediction of temperature is attributed to the assumption of thermal equilibrium which leads to a more rapid voiding of the heated sections in the predictions.

The final step in the verification of the RAMA code will be achieved with the RD-14 loop (see Figure 9 and Table 3). With a single heated section in each pass of the figure-of-eight circuit, experiments at operating conditions close to those of a CANDU reactor in terms of heat flux, fuel channel mass flow rate, and elevation change will be possible. To achieve an event sequence similar to that expected in a CANDU reactor during a LOCA, volumes for circuit components, stored heat and coolant transit time have been scaled on a per channel basis. The result is a pressurized water loop with centrifugal pumps similar to reactor pumps, but smaller in size; U-tube steam generators of the recirculating type with 44 full-length tubes; full-size flow tubes containing 6-m long bundles of 36 electrically heated rods; and a representative high-pressure water injection system. Experiments using this loop are expected to start during 1984.

FUEL ELEMENT BEHAVIOUR

A CANDU-PHW fuel element consists of uranium dioxide pellets encased in a Zircaloy sheath with end caps. The fuel elements operate with collapsed sheaths and to a relatively low burnup. In general, the low burnup and lower temperatures due to low gas-gap resistance mean that only a relatively small mass of volatile fission gases collects in the gas space. Consequently, the sheaths have only to relax a small amount to accommodate large increases in gas temperature and pressure.

Fuel-sheath behaviour during a LOCA is analyzed using the computer code ELOCA and its variants [22]. It assumes one-dimensional heat transfer and deformation and is based on a unified microstructural creep model of Zircaloy at temperatures above 480°C [23,24]. This creep model allows for the interaction of diffusional and dislocation creep with changes in material microstructure expected during a LOCA. Other factors affecting deformation and failure of fuel sheaths are also included, such as:

(i) non-uniform material structure, resulting from temperature variations along or around the fuel sheath;

(ii) oxidation of the fuel sheath above 900°C, which strengthens the sheath and reduces deformation;

(iii) cracking of the oxide layers and the resulting localized strain;

(iv) failure at large strains;

(v) failure by beryllium-assisted cracking near fuel-sheath spacers and bearing pads.

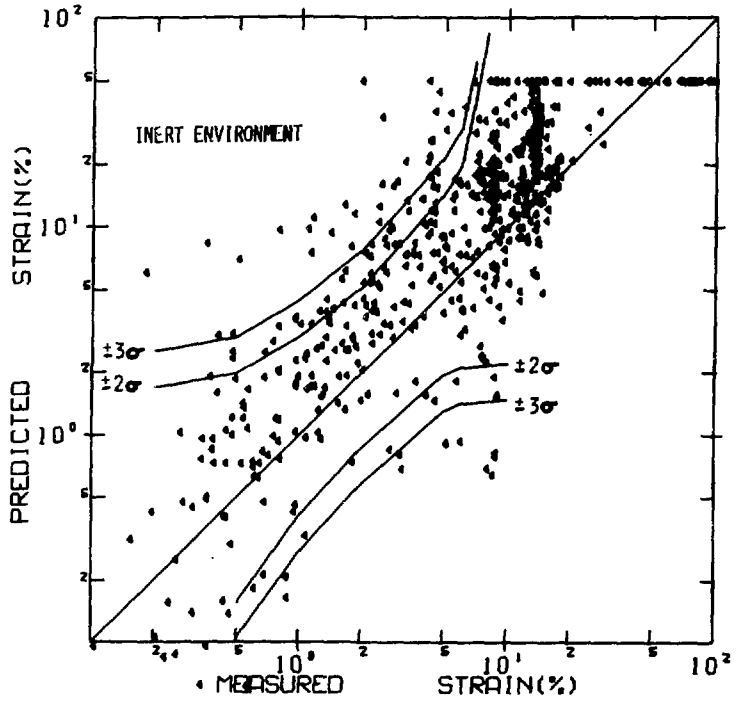

FIGURE 11: Comparison Between Measured and Predicted Values of Strain for Zircaloy Tubes Strained in an Inert Atmosphere

Figure 11 shows a comparison between measured and predicted strains for over 700 experiments on Zircaloy tubes strained in an inert atmosphere. The lines labelled 2σ and 3σ represent limits due to experimental uncertainty: temperature measurement accuracy, wall thickness variations, and the like. As evident, the agreement between model and experiment is generally within the experimental uncertainty. Similar agreement has been achieved between prediction and experiments in which Zircaloy tubes were strained in an oxidizing environment [25].

A sheath-failure model has been developed for the temperature range 600°C to 1300°C [26]. The model assumes that the deformation of the tube is controlled by steady-state creep and that there is a relationship between the tangential stress and the temperature at the instant of failure. For a prescribed pressure and temperature sequence, the steady-state creep rate is integrated numerically to provide the tangential strain and stress as a function of time. Failure is assumed when the tangential stress reaches the value given by an empirical equation relating tangential stress and temperature at failure. The model also allows for circumferential variations of temperature, assuming that the thin-walled sheath is a membrane.

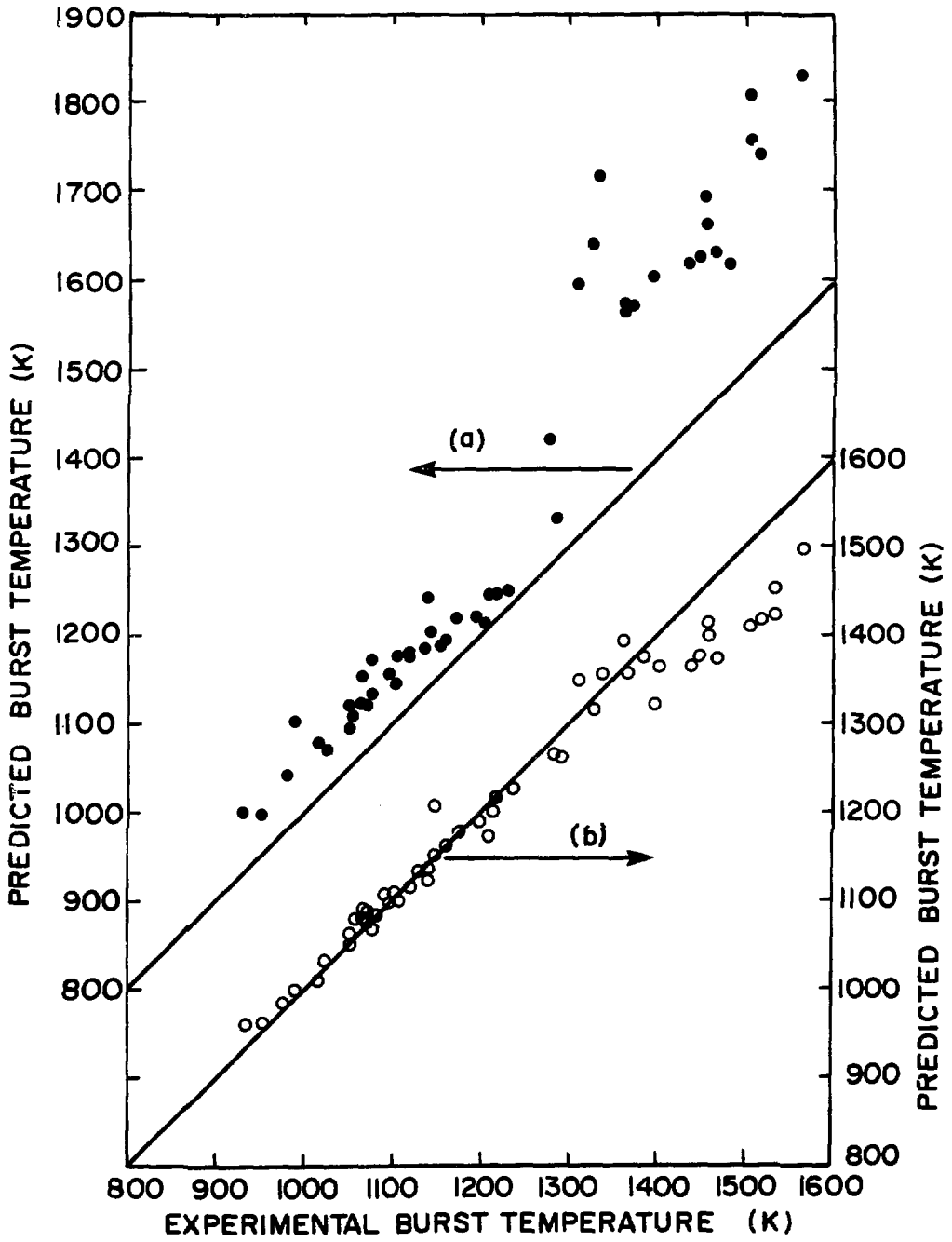

FIGURE 12: Comparison of Measured and Predicted Burst Temperatures:
(a) Linear Pressure Variation
(b) Constant Gas Mass

Figure 12 shows a comparison between prediction and experiment for internally pressurized tubes that were subjected to a linear increase in temperature until failure occurred. Since the time variation of the internal pressure was not reported, two assumptions were made:

(a) pressure varied linearly between the measured initial and burst pressures;

(b) in cases where the mass of the gas enclosed by the tube was known, the pressure variation was calculated using the ideal-gas equation.

As evident, the agreement between experiment and prediction is best when the assumption of constant mass is made. However, the difference between predicted burst temperatures for the two assumptions is relatively small.

In other experiments, the conditions under which fuel sheaths become embrittled by oxygen have been determined [27]. Sheath specimens were exposed to steam at constant temperatures in the range 1000°C to 1500°C, cooled at varying rates, and then loaded in tension at temperatures between 20°C and 800°C. The results showed that tensile properties were not affected by either the oxidation temperature or the cooling rate. For uniform oxygen distributions exceeding 0.7 weight percent, the specimens were brittle at room temperature. However, in all cases where the oxygen concentration was less than 0.7 weight percent over at least one-half the thickness, the specimens remained intact. This result is the basis for an oxygen-embrittlement criterion.

Figure 13 shows the results of experiments done to verify the oxygen-embrittlement criterion. Fuel element segments (one-third the length of a normal element) were heated inductively in steam at various fixed temperatures and times to achieve a desired oxygen distribution. The specimens were then water-quenched to simulate the effects of rewetting. The presence of sheath defects was determined by a pressure test, and the oxygen distribution determined by microhardness measurements. As evident, the experiments confirm the embrittlement criterion.

To use the oxygen-embrittlement criterion, the oxygen distribution in the fuel sheath must be known. A mathematical model for oxygen diffusion has been developed [28], and is available in the form of a computer code, OXWEX [29]. For a prescribed temperature transient above the alpha/beta transformation temperature, OXWEX treats the formation of an alpha plus beta region and the movements of the region boundaries.

A theoretically based multi-dimensional computer code, FAXMOD [30,31] has been developed to examine spatial effects such as:

(i) circumferential variations of heat generation, pellet-sheath contact and coolant conditions around a fuel element (two-dimensional plane stress or plane strain);

(ii) fuel element end-region geometry (three-dimensional axisymmetric mode);

(iii) sheath appendages and braze zones.

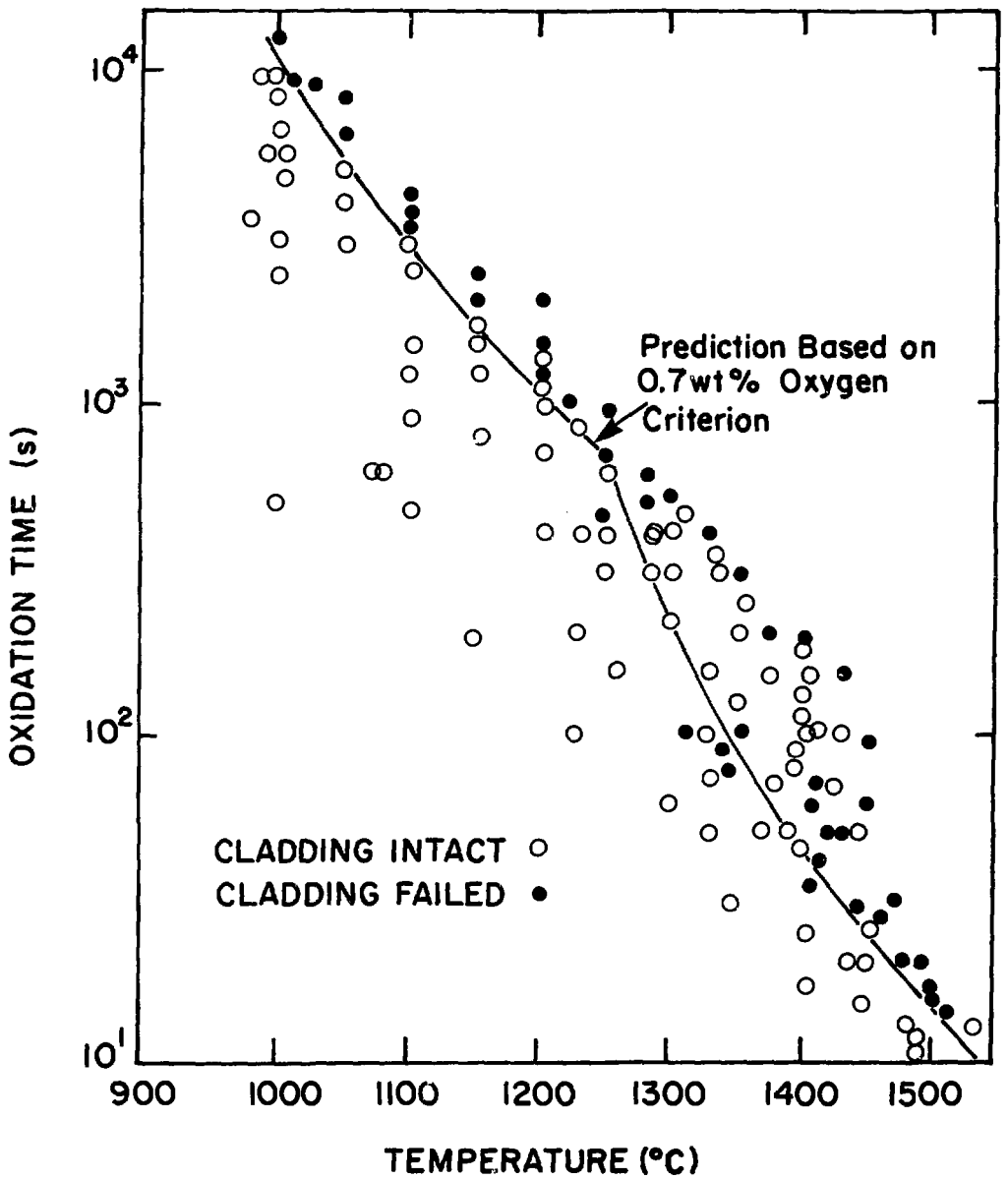

FIGURE 13: Criterion for Oxygen Embrittlement of Fuel Sheaths

FAXMOD consists of two major components: an elastic-plastic and creep analysis, and a non-linear transient thermal analysis. Both analyses are based on the finite-element approach. The formulation allows detailed analyses of multi-dimensional phenomena within a theoretical framework that

can accommodate fundamental material behaviour laws or empirical equations, as appropriate. The required input information includes the initial geometry of the fuel element, material properties (mechanical and thermal) as functions of temperature and irradiation history, and the transient heat generation and coolant boundary conditions to be imposed.

The continuing research associated with fuel element behaviour is focussed on:

(i) experiments with electrically heated, fuel-element simulators to check the FAXMOD code;

(ii) development of a fuel-bundle model that couples fuel-element behaviour to transient heat-transfer and fluid-dynamic processes within the fuel channel;

(iii) in-reactor experiments on standard CANDU fuel elements, arranged in three- and seven-element clusters, to study their behaviour under LOCA conditions, and to study the transport of fission gases that would be released at very high temperatures.

The in-reactor experiments will use the X-9 loop currently being built for installation in the NRX reactor [32]. This loop is designed to:

(i) operate with both superheated steam and sub-cooled water coolant. Operation with superheated steam will provide easily described (relative to those normally associated with transient boiling conditions) surface heat-removal conditions during transients. It will also allow very high fuel sheath temperatures to be reached.

(ii) permit coolant blowdown and subsequent injection of cold water from a gas-pressurized accumulator. This will allow investigations of fuel element thermal-mechanical behaviour under thermalhydraulic conditions representative of LOCAs.

(iii) permit the full inventory of volatile fission products to be released from the fuel elements. This will allow fission-product chemistry and transport studies to be done at very high temperatures.

Experiments are expected to start in 1984 July.

FUEL CHANNEL BEHAVIOUR

Background

If there is a LOCA, and simultaneous failure of the ECI system, the maximum fuel-channel temperatures would be limited by heat transfer to the cool moderator water that surrounds each channel (see Figure 14). Because the fuel is separated from this water only by the relatively thin pressure and calandria tubes, it cannot simultaneously become very hot and remain insulated from the water.

The sequence of events during heat-up is shown schematically in Figure 14. Initially heat is transferred by radiation from the fuel to the pressure tube and calandria tube, and then to the moderator water by convection. The resulting fuel and pressure-tube temperatures are sufficiently high to initiate a chemical reaction between zirconium and steam that produces more heat and liberates hydrogen gas. Also, more of the volatile fission products diffuse out of the fuel pellets. As the pressure tube heats up, it deforms into contact with the calandria tube. If the internal pressure is low, the pressure tube sags into contact (at about

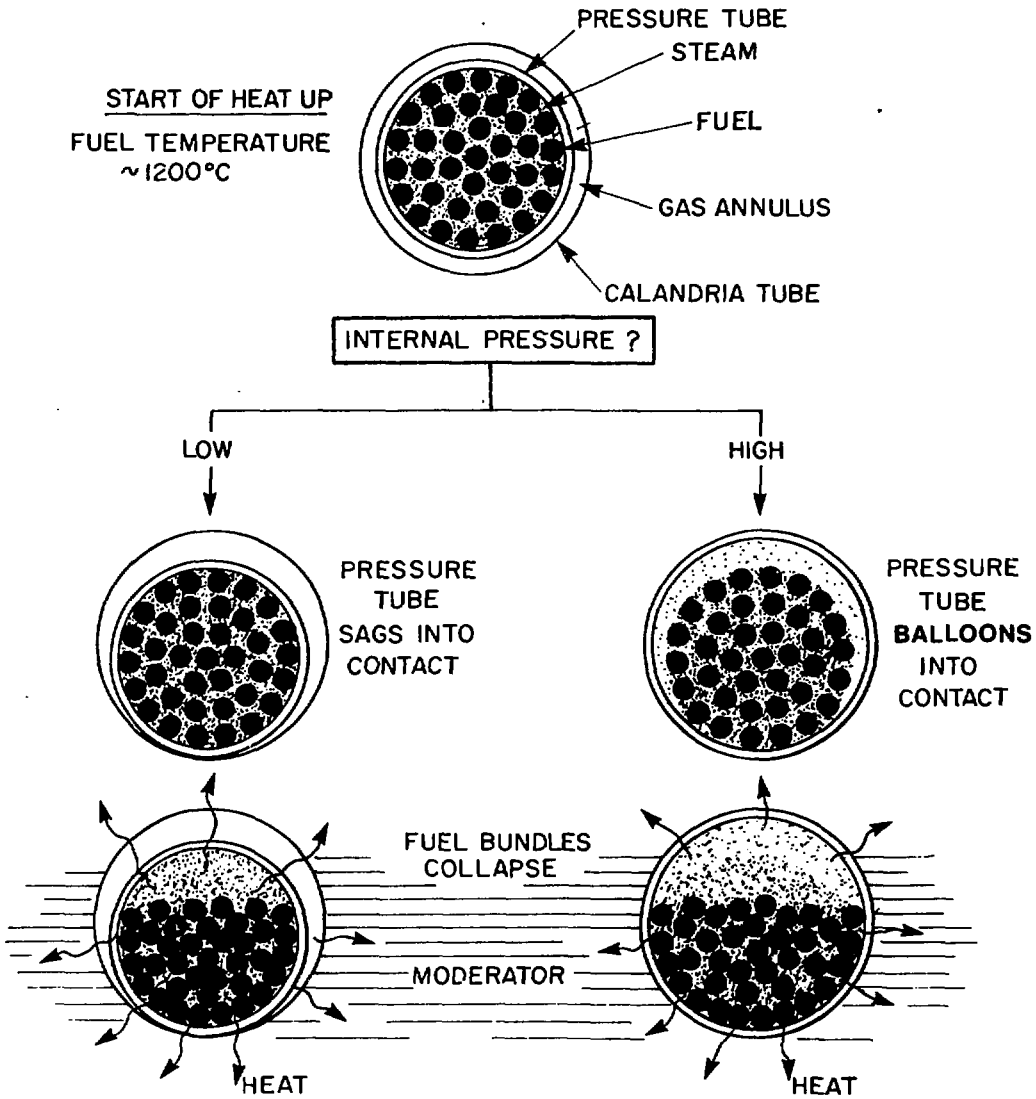

FIGURE 14: Schematic of the Stages of Fuel Channel Heat-Up and Deformation

1000°C) under the weight of the fuel; if the pressure is high it deforms radially (balloons) into contact (between 650°C and 1050°C depending on the internal pressure and the heat-up rate).

Upon contact there is a peak in the heat flux at the calandria-tube surface caused by the sudden release of stored heat from the pressure tube. The rate of release is affected by the magnitude of the contact conductance at the interface between the pressure and calandria tubes, and by the mode of boiling heat transfer at the outer surface of the calandria tube. The important question at this point is: Is the rate of heat transfer to the moderator sufficient to prevent further deformation of the pressure and calandria tubes?

Heat transfer from the fuel is relatively unaffected by the contact between the pressure and calandria tubes. At about 1500°C the fuel-bundle elements slump into contact so that heat transfer within the fuel and from the fuel to the pressure tube will have a large conduction component. Here the important question is: Does any fuel melt?

Thermal Analysis

The computer code CHAN [33] has been developed to calculate fuel-channel temperature transients during heat-up. In CHAN, the fuel channel is represented by axial segments, each one fuel bundle in length. Within each segment the fuel bundle is represented by a series of annular rings. This simplification results in higher inner-element temperatures than a more precise treatment of element-to-element heat transfer. However, it is unlikely that the initial geometry will be maintained throughout the transient, and the annular representation is thought to be more realistic. Allowances are also made for:

(i) heat and hydrogen produced by the zirconium-water reaction that occurs at high temperature [34];

(ii) heat convected to the mixture of steam and hydrogen flowing axially through the annuli;

(iii) contact between the pressure and calandria tubes at a specified temperature (obtained from an independent mechanical analysis) and the resultant boiling heat transfer at the outer surface of the calandria tube [35]. Two modes of contact are considered: contact over a segment of the inner surface of the calandria tube caused by sag of the pressure tube under the weight of the fuel, and uniform circumferential contact caused by the radial deformation of the pressure tube under uniform internal pressure;

(iv) the contact conductance between the pressure and calandria tubes. The contact conductance (obtained from experiments using pressure- and calandria-tube specimens) determines the rate of release of stored heat from the pressure tube.

Figure 15 shows temperature histories and the heat-flux transient at the calandria-tube surface, calculated using CHAN, for a fuel channel with high internal pressure. We have assumed the steam flow rate for the fuel channel that produces the highest temperatures, i.e. just the right amount of steam to fuel the zirconium-water reaction, but not enough to convect any

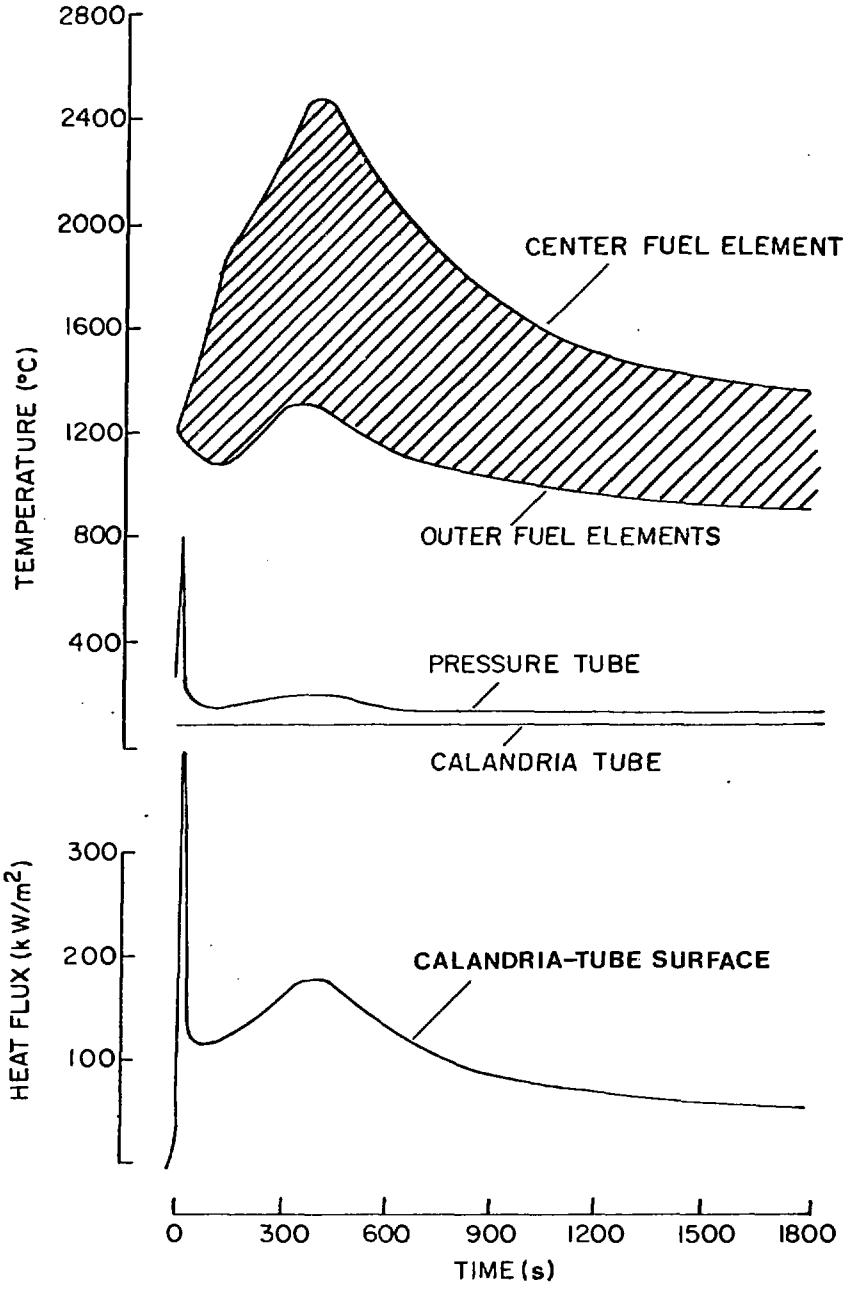

FIGURE 15: CHAN Predictions for Fuel Channel Heat-Up with High Internal Pressure: Hottest Channel Position

heat away. As can be seen from the figure, the pressure tube is predicted to balloon into contact with the calandria tube at 800°C, and it is assumed the nucleate boiling on the calandria tube surface is not disrupted. The peaks in the temperature histories and surface heat flux, at about 400 s, indicate that the zirconium-water reaction has reached its maximum rate. It can be seen that the maximum fuel temperature does not exceed the melting temperature of UO_2 (2800°C). We conclude that, even in the worst case, there will be no fuel melting.

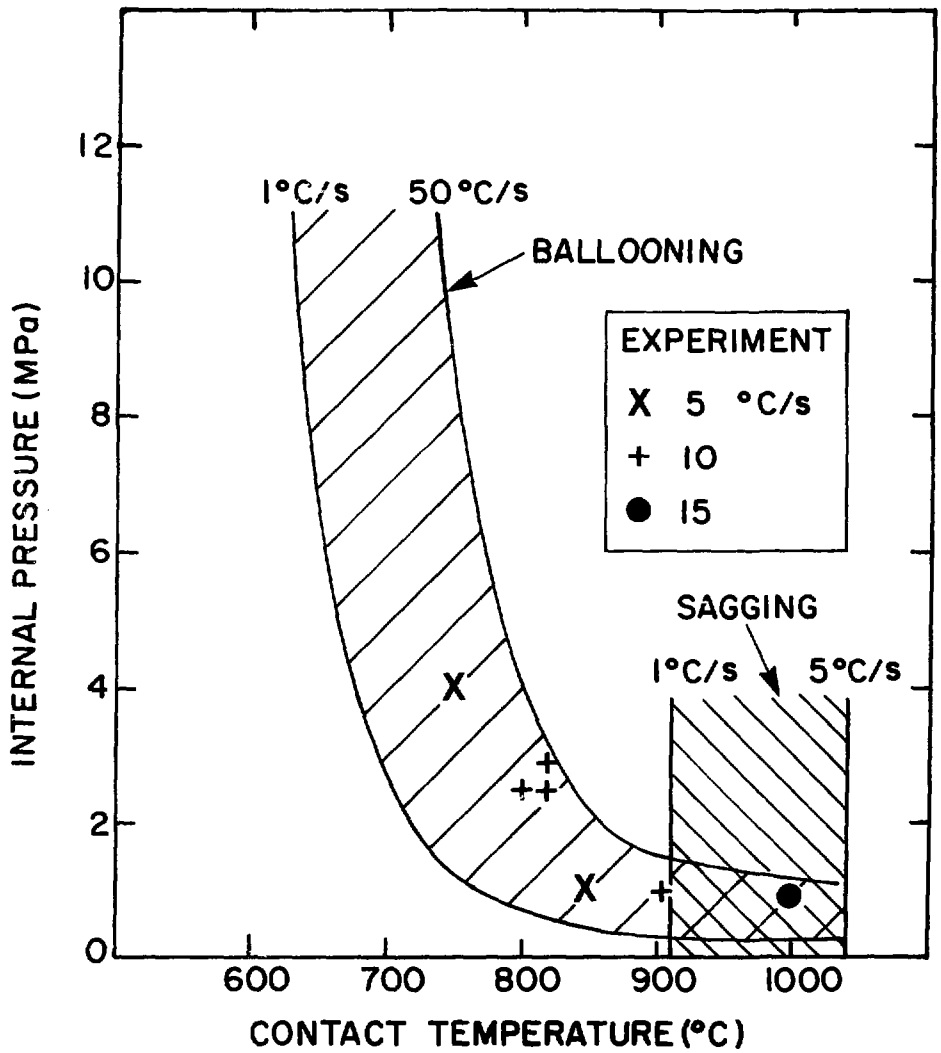

FIGURE 16: Pressure-Tube Contact Temperature as a Function of Internal Pressure and Temperature Rise Rate

Mechanical Analysis

Pressure-tube deformation is predicted using one-dimensional deformation models, empirical equations for the strain rate, and specified pressure and temperature transients (obtained from CHAN). For pressure-tube sag, a computer code has been developed [36] that solves a one-dimensional beam equation with uniform axial load. The strain-rate equations have been derived from isothermal tensile tests on longitudinal pressure-tube specimens. For pressure-tube ballooning, a simple one-dimensional radial deformation model is used [37]. To account for the anisotropy of the material, transverse pressure-tube specimens are used to derive the strain-rate equations. Allowance is also made for micro-structural effects, such as grain growth. This is necessary because transient strain rates calculated using equations derived from isothermal tensile tests (where grain growth is essentially complete) are lower than those measured on internally pressurized, rapidly heated (15°C/s) pressure-tube segments (where there is little or no growth). Two-dimensional deformation models have also been developed to analyze the effects of circumferentially nonuniform temperature distributions that might develop due to nonuniform contact between the pressure and calandria tubes.

Figure 16 shows contact temperature as a function of internal pressure for selected values of the pressure-tube temperature-rise rate. The curves were calculated using the above methods. Also shown are values of contact temperature measured during experiments on internally pressurized pressure-tube segments. The experiments are described below. As evident, the pressure-tube contact temperature can be expected to lie in the range 650°C to 1050°C.

Experiments

To check the empirical strain-rate equations under transient conditions, the deformation of transverse and longitudinal pressure-tube specimens has been measured while they were held under constant load and heated to produce a constant rate of temperature rise. Typical results are shown in Figure 17 for a transverse specimen with a temperature-rise rate of 5°C/s. Prediction and experiment are in good agreement. In other experiments, the radial deformation of internally pressurized segments of pressure tubes has been measured for controlled temperature transients. Agreement between experiment and prediction is again good.

Figure 18 is a schematic of an experimental apparatus used to study the combined mechanical and thermal processes associated with a hot pressure tube ballooning into contact with a cooled calandria tube. A full-size segment of a pressure tube can be heated at rates up to 15°C/s by radiation heat transfer from an internally located electric heater, and pressurized to 4 MPa with helium gas. The temperature of the water pool can be controlled between 70°C and 90°C.

The results from a series of experiments with this apparatus are shown in Figure 19 [37,38]. Heating rate, internal pressure and water temperature were varied to get the desired contact and heat-transfer conditions. In the

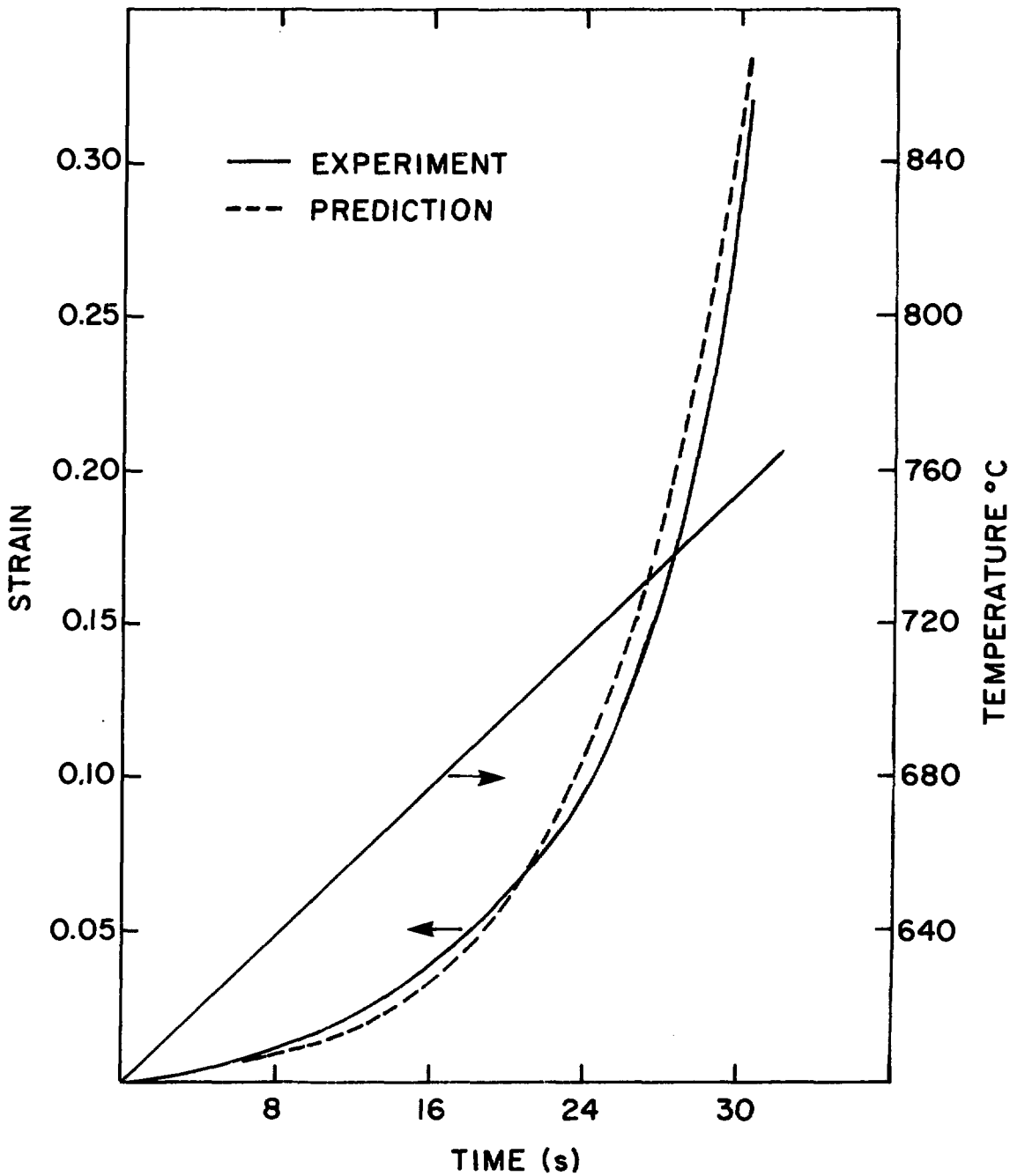

FIGURE 17: Measured and Predicted Strain Transients for a Pressure-Tube Specimen under Constant Load and Temperature-Rise Rate

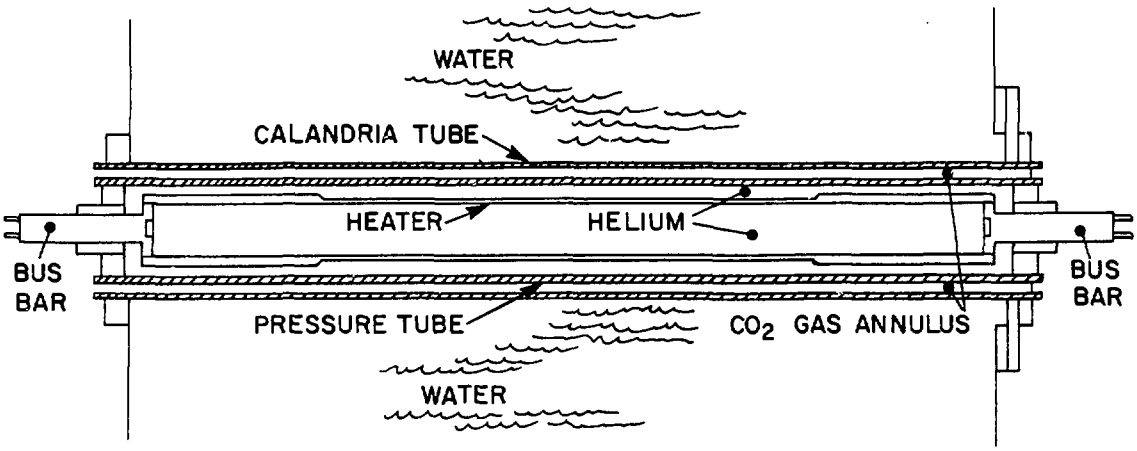

FIGURE 18: Experimental Apparatus Used to Study Heat Transfer and Deformation

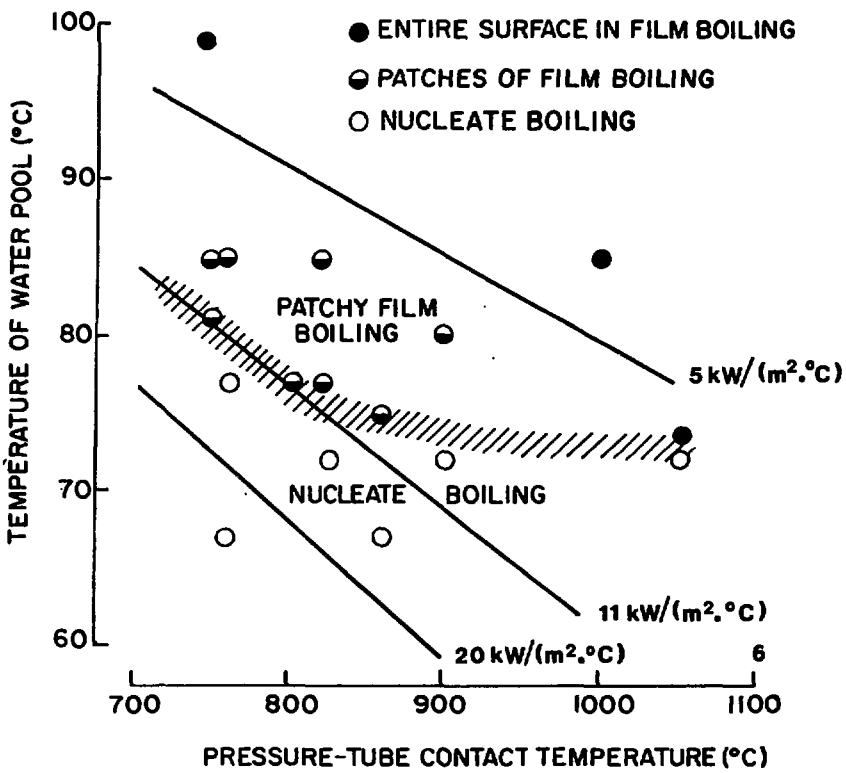

FIGURE 19: Summary of Surface Boiling Conditions for Various Contact and Water Temperatures

figure, nucleate boiling and film boiling heat transfer are denoted by open and solid symbols, respectively. The half-solid symbols denote a mixture of nucleate and film boiling. The solid lines are the loci of conditions needed to initiate film boiling as predicted by the computer code WALLR [37]. It solves the radial heat-conduction equation using a finite-element method, including allowances for the contact conductance between the pressure and calandria tubes and the nature of the boiling process at the calandria-tube surface. Each line corresponds to a specific value for the contact conductance. Other experiments, using pressure- and calandria-tube specimens, indicate that the contact conductance is about 11 $kW \cdot m^{-2} \cdot °C^{-1}$ with a moderate contact pressure. The agreement between prediction and experiment is seen to be good at the lower contact temperatures (high contact pressures), but the sub-cooling required to avoid film boiling is over-predicted for higher contact temperatures (low contact pressures). This is likely caused by the reduced contact conductance resulting from decreased contact pressure, which is not allowed for in the prediction. Experiments to investigate this point are underway.

Figure 20 shows pressure- and calandria-tube temperature transients measured during an experiment in which the heat release from the pressure tube upon contact resulted in film boiling over most of the calandria-tube surface. Although the internal heat production rate was maintained, the vapour film gradually collapsed, rewetting the calandria-tube surface with an attendant sharp drop in temperature to about 100°C. The dashed line is a prediction of the calandria-tube temperature made with WALLR, using a heat-transfer coefficient of 400 $kW \cdot m^{-2} \cdot °C^{-1}$ (determined from independent film-boiling experiments). It is in good agreement with the experiment up to the point of film collapse and rewetting. These phenomena are not included in the model and are subjects of continuing research. It is encouraging to note that, even under the severe conditions of this experiment, only minor deformation of the calandria tube was observed.

To check the thermal and mechanical analyses associated with pressure-tube sag, experiments are being done with the apparatus shown in Figure 21. The pressure- and calandria-tube segments are 3 m long. The pressure tube is rolled into steel hubs at both ends to provide representative support conditions and contains a ring of electrical heating elements that contact its inner surface. The remaining space is filled with a thermal insulating material and steel pellets, providing a uniformly distributed load of 60 kg/m to simulate the effect of the fuel bundles. The arrangement shown in the figure provides pressure-tube temperature-rise rates up to 6°C/s. The temperature of the water pool surrounding the calandria tube can be controlled between 70°C and 90°C.

The first experiments with this apparatus were done to study pressure-tube deformation without the calandria tube and surrounding water pool. Figure 22 shows a typical pressure-tube temperature transient at mid-length. Although the agreement between prediction and measurement is reasonable, we believe it can be improved through use of an improved strain-rate equation.

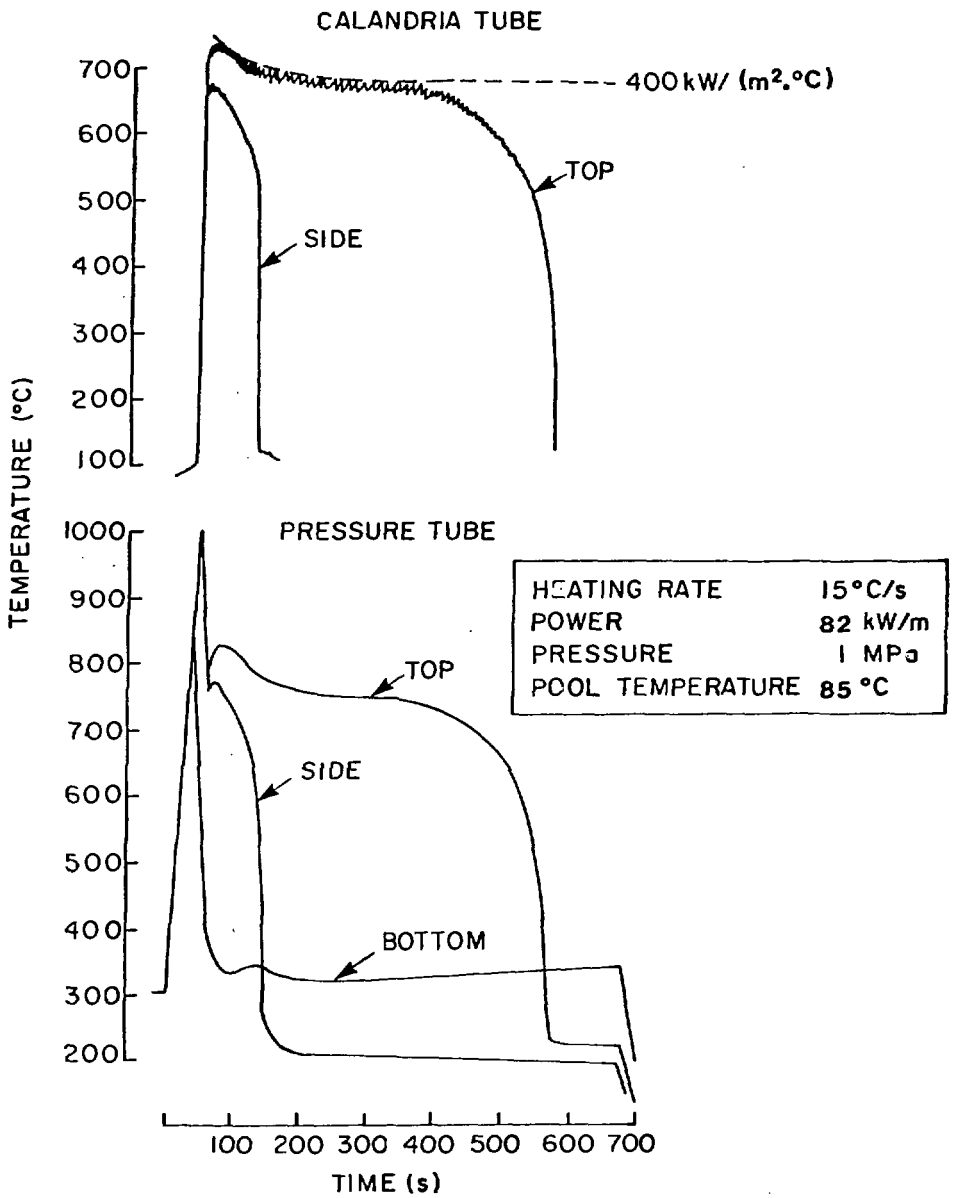

FIGURE 20: Pressure- and Calandria-Tube Temperature Transients Measured during an Experiment with Film Boiling on the Calandria-Tube Surface

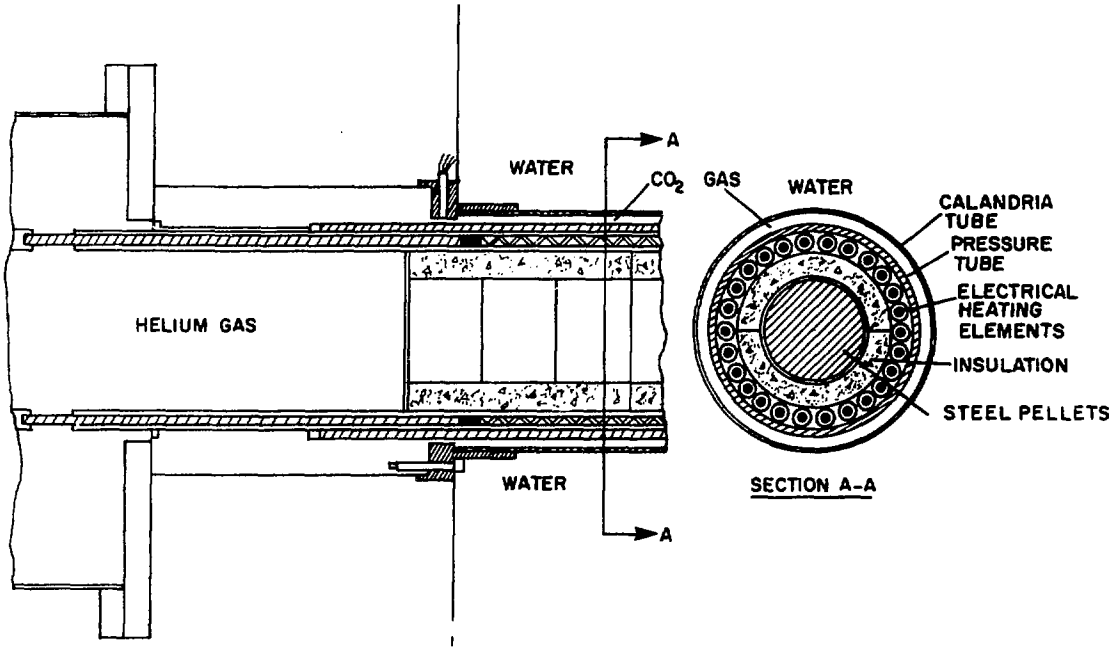

FIGURE 21: Experimental Apparatus Used to Study Heat Transfer and Deformation Processes Associated with Pressure-Tube Sagging

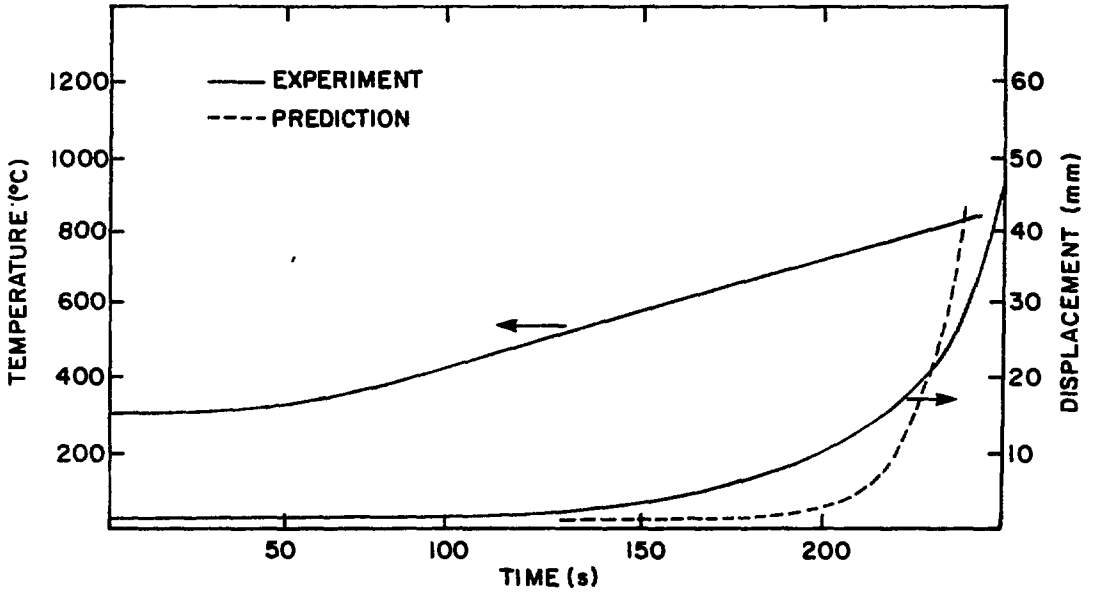

FIGURE 22: Measured and Predicted Displacement Transients for a Uniformly Loaded Pressure-Tube Segment Sagging in Air

The continuing research associated with fuel-channel behaviour is focussed on:

(i) refining the constitutive equations for the strain rate of zirconium alloys at high temperature (including micro-structural effects) and for the thermal contact conductance between the pressure and calandria tubes;

(ii) development of multi-dimensional deformation models to analyze the effects of non-uniform contact between the pressure and calandria tubes and of non-uniform heat removal from the outer surface of the calandria tube;

(iii) experiments on full-size simulated fuel channels to verify fuel-channel deformation models;

(iv) experiments using fuel-element simulators to verify the CHAN code in situations involving chemical reaction between zirconium and steam.

FISSION PRODUCT CHEMISTRY

Figure 23 shows the basic elements of iodine behaviour during a LOCA should fuel sheaths fail. Iodine is released from the fuel into the surrounding fluid (most likely highly superheated steam), transported with this fluid to the break, and then discharged into the reactor building. In the reactor building, iodine partitions between the gas and solution phases depending on the chemical forms present. Iodine behaviour therefore depends critically on the chemical conditions encountered and, because iodine is highly reactive, several chemical forms could be present.

Previously it was assumed that large quantities of iodine would enter the gas phase. Experience from the Three Mile Island accident shows that, even though a large fraction of the iodine inventory was released from the fuel, airborne iodine concentrations were very small. This emphasizes the complex behaviour of iodine, but more importantly it shows that there are opportunities to identify processes to ensure that iodine will be trapped in the containment system.

We believe that recent fundamental studies [39,40] have increased our understanding of iodine behaviour to the point where large gains in safety-system performance are possible. Based on these studies, we are able to provide a tentative description of the chemistry conditions favourable to trapping iodine in solution. They appear to have been met during the Three Mile Island accident, and allow a plausible explanation of what happened. In addition, the understanding gained suggests that there may be a variety of simple means to enhance the naturally occurring trapping processes.

Iodine is probably released from the fuel as CsI vapour and its subsequent behaviour depends on the conditions it encounters. The most

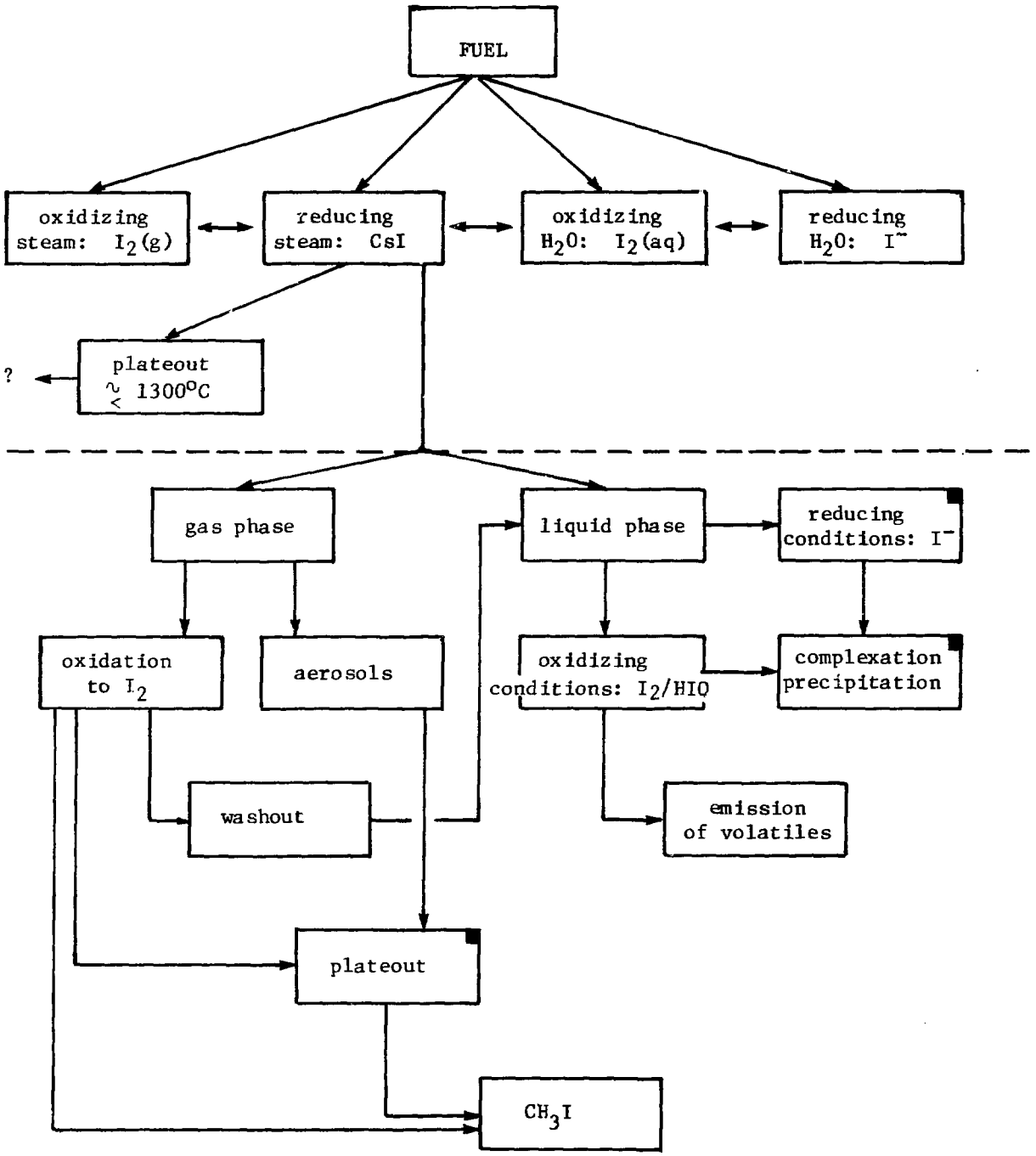

FIGURE 23: Basic Elements of Iodine Chemistry

likely environment is reducing or slightly oxidizing steam, wherein CsI is stable and will be transported with the steam. Below 1300°C, some CsI will plate out on surfaces and it will only be removed if oxygen, or water, is present. If the steam-CsI mixture condenses, iodine will be instantly converted to highly involatile I^-. If CsI encounters water in the PHT system, the same reaction will occur under the oxidation potential and pH conditions likely to prevail.

Figure 24 shows a Pourbaix diagram which summarizes the predominant iodine forms for a range of possible chemistry conditions. It is a plot of oxidation potential (a measure of the amount of oxygen dissolved in the water) versus pH (the acidity of the water) for a total iodine concentration of 10^{-9} mol·dm^{-3} and water temperature of 100°C. To prepare the diagram, the chemical behaviour of iodine at 25°C was extrapolated using thermodynamic models. The dashed lines are the stability limits for water: the top dashed line corresponds to oxygen-saturated water while the bottom line corresponds to hydrogen-saturated water. The major volatile forms (I_2, HOI) are found in the upper left-hand corner, corresponding to

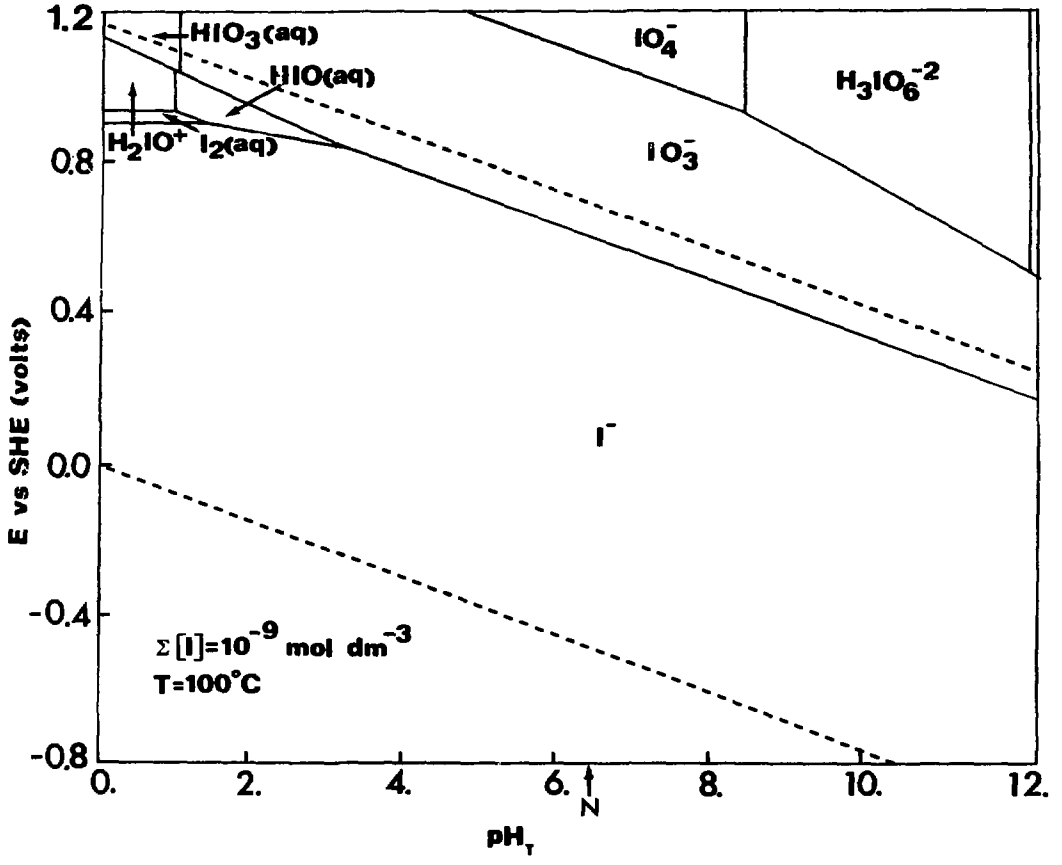

FIGURE 24: Pourbaix Diagram for Iodine Solution Forms

highly acidic and oxidizing conditions. Basic or reducing conditions favour formation of highly involatile I^-. There are simple additives that can maintain these conditions and, in addition, there may be other simple species that can complex the iodine.

The concentration of iodine in the gas phase in equilibrium with an aqueous solution depends on the concentration of I_2 and HOI in the solution. Speciation is affected by factors such as temperature, pH, oxidation potential, concentration, and the presence of other species that might form complexes or precipitates with iodine. The exact distribution of iodine among the various aqueous and gaseous forms can be calculated by simultaneously considering the equilibrium constants for all possible reactions. Figure 25 shows the variation of the partition coefficient as a

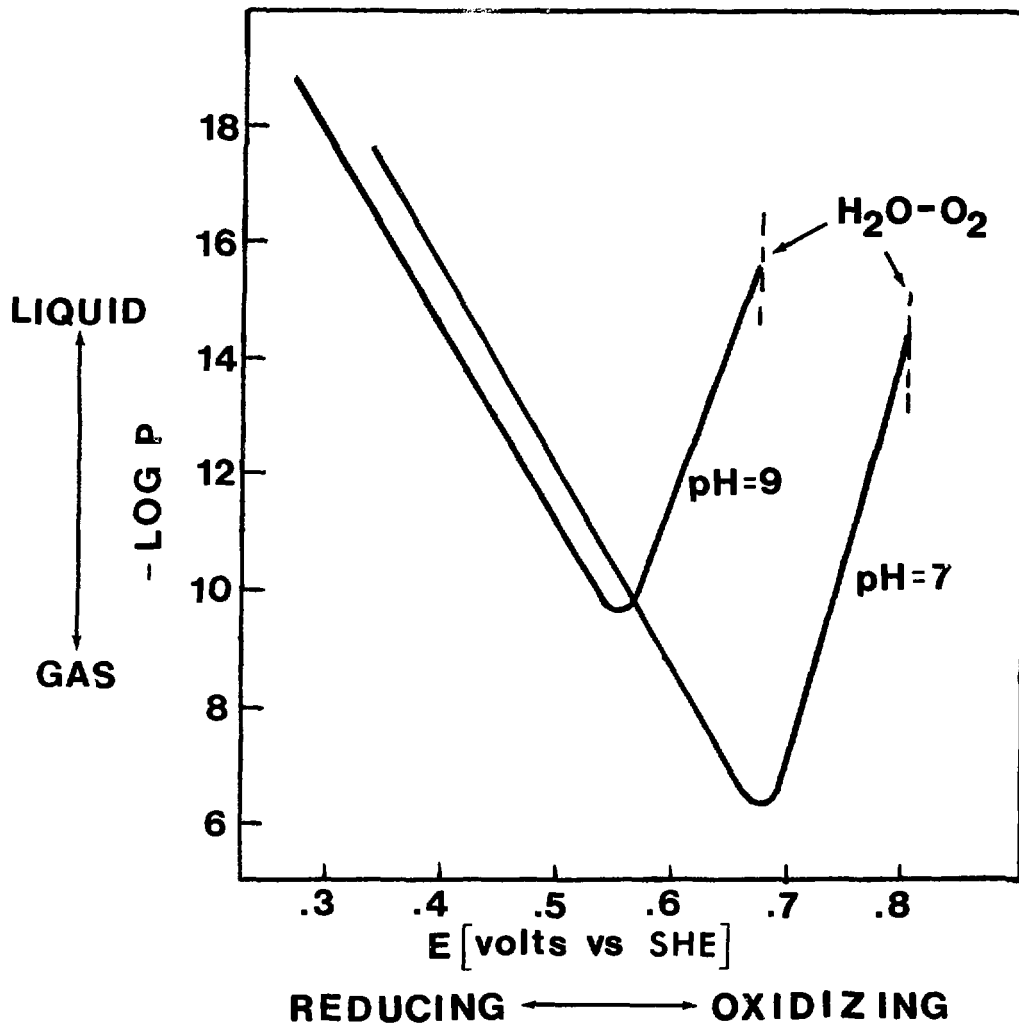

FIGURE 25: Aqueous/Gas Partition Coefficients for Iodine

function of oxidation potential for pH 7 and 9. Under highly oxidizing conditions (air-saturated water), the partition coefficient is relatively large. As the oxidation potential decreases, the partition coefficient decreases, passes through a minimum, and then increases sharply. The conditions that minimize equilibrium transport of iodine from aqueous solution to the gas phase are: low temperature, low concentration, high pH, and a strongly reducing medium. If these conditions are maintained, partition coefficients of 10^{+12} to 10^{+16} are possible. For example, if a 10^{-6} mol·dm^{-3} solution of iodine corresponds to 10^{7} Ci (1 Ci = 37 GBq), then only 10 Ci would be found in the gas phase under the worst oxidation condition at pH 7, where the partition coefficient is 10^{6}.

If conditions are chosen so that inorganic iodine volatility is small, then methyl iodide (CH_3I) becomes the dominant airborne species. Measurements at Three Mile Island indicate that CH_3I made up 80 to 90 percent of the airborne iodine following the accident. The origin of CH_3I is not well understood, nor is its chemistry once it is formed. Neither water sprays nor surface deposition are effective in fixing CH_3I, and other means must be sought. Electrochemical techniques are being investigated.

Although experimental verification is needed, analyses of iodine behaviour during LOCA conditions suggest that airborne iodine concentrations should be extremely small if appropriate chemistry conditions are maintained: low temperature, low concentration (i.e. large quantities of water), high pH, and low oxidation potential. These conditions are expected to be present.

The continuing research on iodine chemistry is focussed on:

(i) experiments and analyses to determine the processes leading to the formation of organic iodine compounds;

(ii) experiments to verify predictions of volatility of various iodine species under conditions appropriate to LOCA situations;

(iii) gas-phase reactions that might be used to reduce airborne concentrations of organic iodine species;

(iv) determining important reaction rates involving iodine species in the primary heat-transport and containment systems.

COMBUSTION OF HYDROGEN-AIR-STEAM MIXTURES

If the fuel and pressure tube become sufficiently hot, hydrogen produced by the zirconium-water reaction mixes with steam in the heat-transport system and is discharged through the break to the reactor building where it mixes with air and more steam. The mixture composition depends on the particular accident scenario. For example, a bounding analysis involving 190 channels would predict a uniform concentration of 4% hydrogen in a 600-MWe CANDU reactor building.

An upper bound for the pressure produced by combustion may be calculated from classical thermodynamics, assuming an adiabatic, constant-

volume process. For a stoichiometric mixture of hydrogen and air (30% hydrogen, 70% air) initially at atmospheric pressure, the peak pressure would exceed eight atmospheres (0.8 MPa). When ignited, the heat produced by the exothermic reaction drives a combustion wave through the mixture. In lean mixtures (hydrogen concentrations less than 10%), which are of interest in containment systems, non-adiabatic processes compete with the combustion wave propagation, and dissipate energy. Flammability limits and incomplete combustion result. The competing processes include:

- buoyant convection;
- heat transfer to walls;
- selective diffusional mixing of reactants.

Figure 26 illustrates the effect of these non-adiabatic processes on the combustion of lean hydrogen-air mixtures. Consider an initially spherical flame kernel. The buoyant velocity is normal to the flame front at the top of the sphere and, hence, upward propagation of the flame is enhanced. At other points in the upper hemisphere, the buoyant acceleration is reduced by the cosine of the angle between the surface normal and the vertical buoyant velocity vector. The net effect is to maintain spherical curvature in the upper hemisphere as the kernel expands and rises. For downward propagation, on the other hand, the buoyant velocity opposes the flame front velocity. Buoyancy therefore decelerates propagation in the lower hemisphere of the flame kernel. The net effect is to reduce curvature and produce a flattened flame front. As the kernel expands, its downward propagation tends to be cancelled by the buoyant rise velocity.

In a large volume containing a lean mixture, the fireball propagates slowly upward and horizontally as its center of mass rises at the buoyant velocity. If the mixture is lean enough, on reaching the top of the volume, the fireball loses heat by conduction and convection to the walls, and cools.

When there is no downward propagation, most of the mixture remains unburned, and the pressure rise is lower than would be expected for an adiabatic process. Pressure rise as a function of hydrogen concentration is shown in Figure 26 for three different experimental configurations [41]. Note the large departures from the ideal adiabatic-combustion process.

Figure 27 shows the results of experiments using a 2-litre vessel (with the ignition source at the bottom) to determine the completeness of combustion for low concentrations of hydrogen in air and air-steam mixtures [42]. Although the data are scattered, the fraction of hydrogen burned appears to decrease only slightly when steam is added. Combustion does not occur for hydrogen concentrations less than 4%, and all of the hydrogen is consumed when its concentration is greater than 10%. These experiments also showed that, although the fraction of hydrogen burned is only slightly affected, the combustion rate is reduced by adding steam.

To extend these results to reactor containment systems, mathematical models are being developed [43]. These models are derived from the

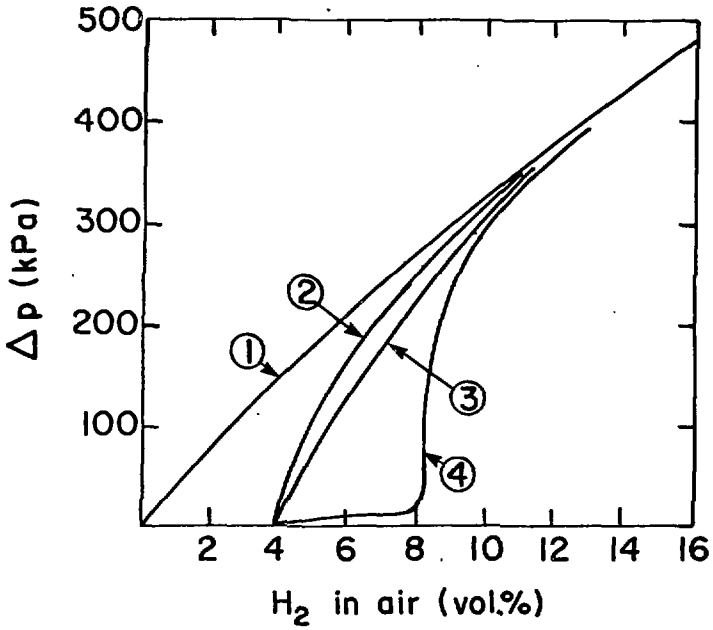

① Adiabatic

② 2-litre chamber with bottom ignition

③ 8-litre chamber with a fan to generate turbulence

④ 4-m diameter sphere with central ignition

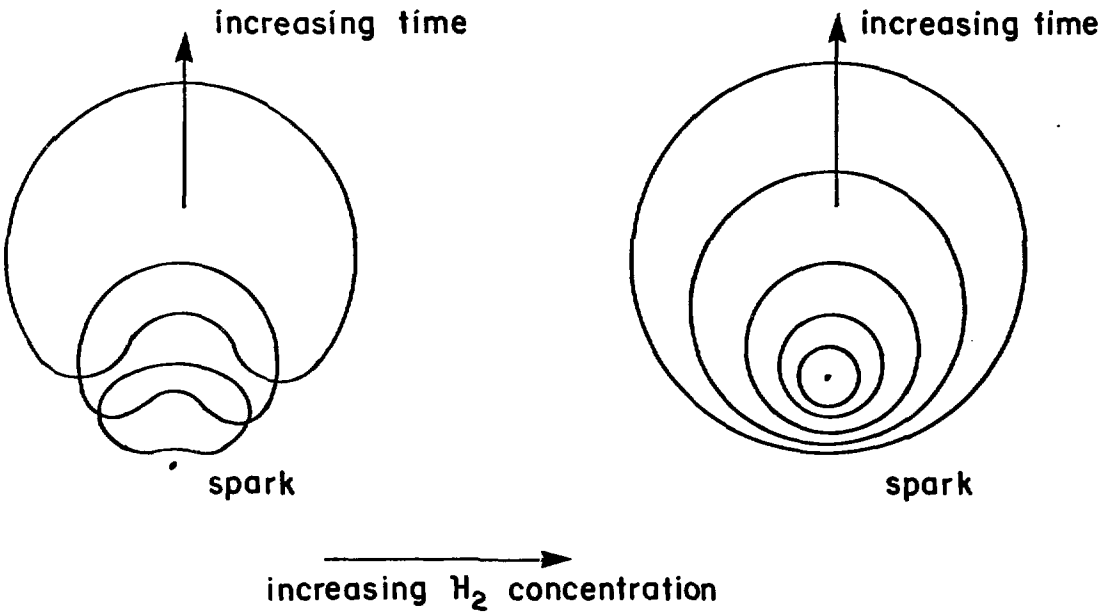

FIGURE 26: Combustion of Lean Hydrogen-Air Mixtures

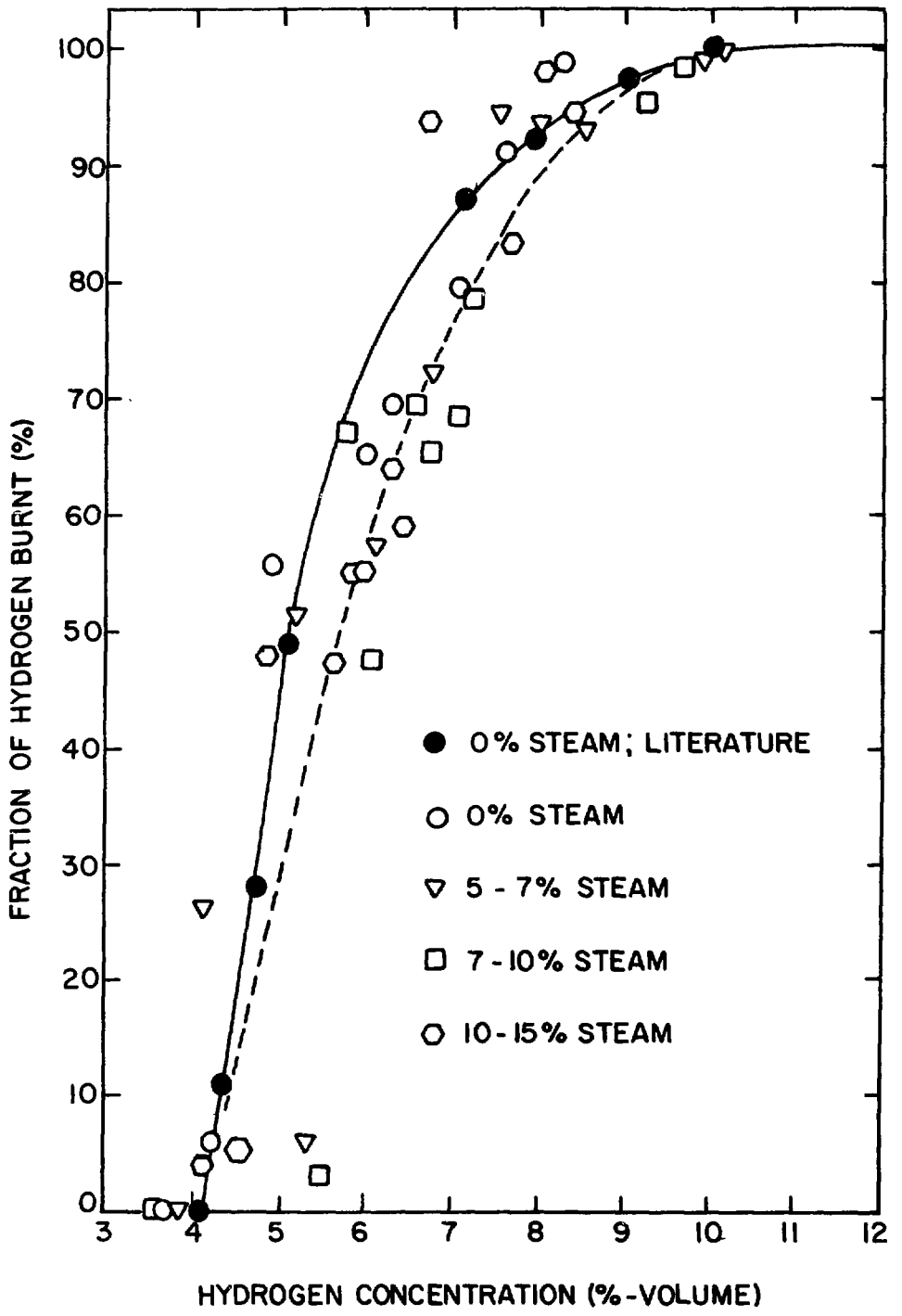

FIGURE 27: Completeness of Combustion in Hydrogen-Air-Steam Mixtures

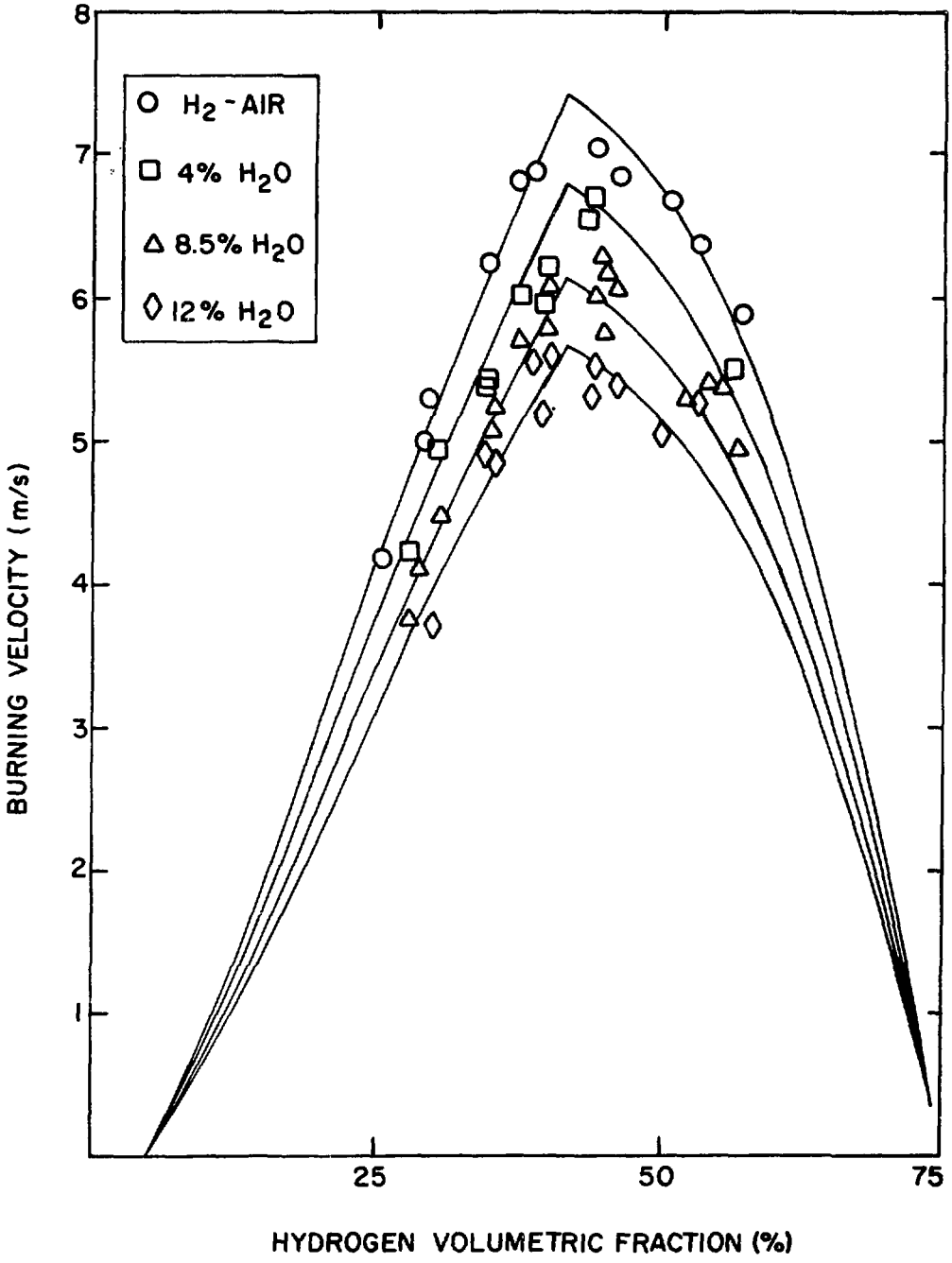

FIGURE 28: Effect of Steam on the Burning Velocity of Hydrogen-Air-Steam Mixtures at 200°C

differential equations for mass, momentum and energy conservation in one dimension, assuming spherical symmetry. The constitutive equations for the combustion rate have been derived from measurements of burning velocity, using a nozzle burner and hydrogen-air-steam mixtures of varying composition [44]. Typical results for a mixture temperature of 200°C are shown in Figure 28. It has been found that the combustion rate increases with the temperature of the unburned mixture, and the burning velocity at 200°C is almost twice that measured at room temperature. As noted above, the burning velocity (combustion rate) is reduced by adding steam. This means that the rate of pressure rise during combustion is reduced when steam is present.

Improved constitutive equations, which include the effects of pressure and turbulence, are the focus of continuing research. Experiments are underway to investigate the combustion of hydrogen-air-steam mixtures in a constant-area duct, leading to turbulent flames. The continuing development of the model is focussed on geometries that are more representative of vacuum containment systems, i.e., systems of large volumes and interconnecting ductwork.

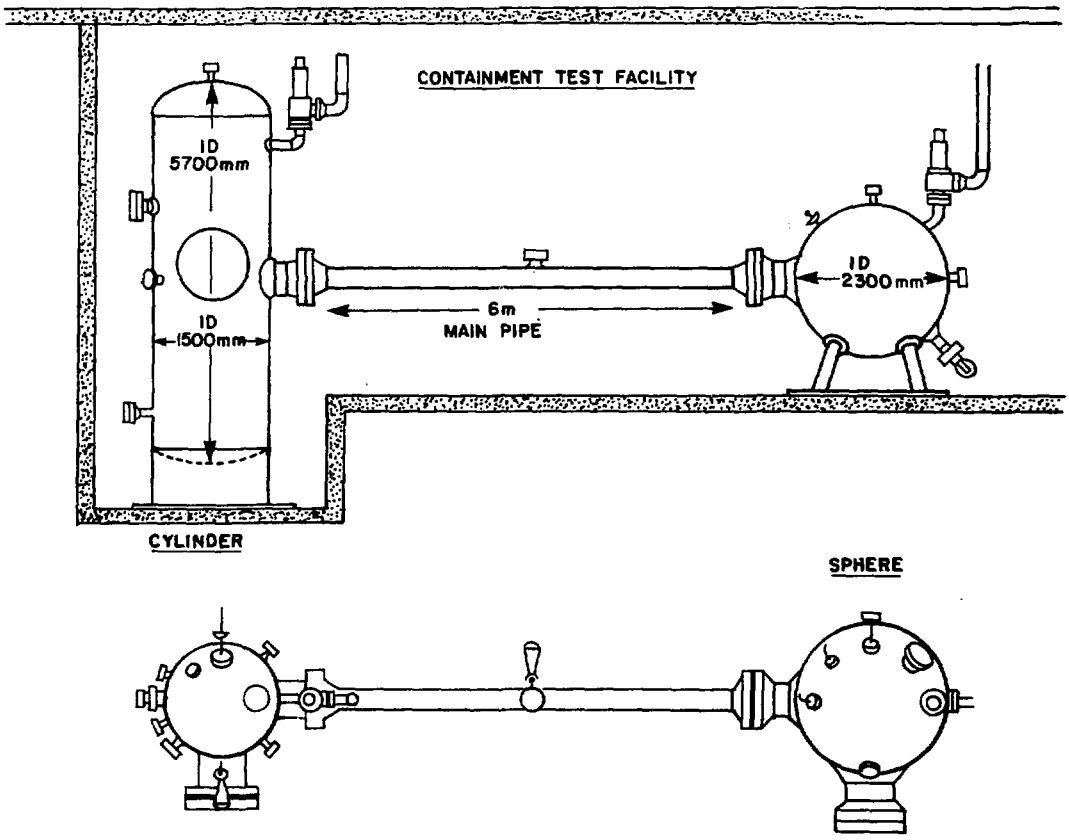

FIGURE 29: Schematic of the Containment Test Facility

Figure 29 shows a schematic diagram of the Containment Test Facility in which the first large-scale hydrogen combustion experiments have been completed [45]. The basic configuration consists of two volumes, a 6.3-m^3 sphere and a 10.3-m^3 cylinder, connected by a duct of variable length and diameter. The components are designed to withstand a pressure of 10 MPa to allow experiments with detonation. The first experiments are being done in the sphere, and other components (duct, cylinder) will be added in stages of increasing complexity. Initially, we are focussing on the combustion of lean mixtures (4% to 10% hydrogen) to provide comparisons with data obtained from the small-vessel combustion experiments described above.

SUMMARY

The research completed to date provides a high degree of assurance that the safety objectives of the CANDU-PHW design have been achieved. Specifically, it has been shown that:

(i) existing computer codes for predictions of thermalhydraulic processes during LOCAs can be used with confidence for a wide range of conditions. Blowdown and refilling experiments confirm that the simplest flow-boiling model (the EVET, or homogeneous equilibrium model and its variants) provides accurate predictions as long as the steam and water remain mixed. The predictions are uncertain for flow situations where the steam and water separate under the influence of gravity and for flow in weakly interacting streams. New models (the UVUT models) are being developed to improve the physical representation of these flows and will be incorporated into the thermalhydraulics codes when complete. In the meantime, the flow conditions at the threshold between the mixed and separated regions have been determined experimentally, allowing the existing models to be used with confidence. Blowdown and refilling experiments in the RD-14 loop, which is similar to a CANDU-PHW PHT system in many important aspects, will provide the final confirmation of prediction accuracy;

(ii) existing models of the thermal and mechanical behaviour of individual fuel elements yield accurate predictions of fuel sheath behaviour for prescribed heat-removal conditions. This includes high-temperature conditions leading to sheath oxidation and embrittlement. Continuing research is focussed on confirming thermal and mechanical behaviour at the very high temperatures associated with conditions following a LOCA and complete failure of the ECI system;

(iii) natural chemical processes are highly effective in retaining in solution any radioiodine that might be released from failed fuel sheaths during a LOCA. This means that airborne concentrations of iodine should be extremely small within the containment system, providing additional assurance of public safety;

(iv) the moderator cooling system ensures that fuel melting will not occur and that fuel-channel integrity will be preserved if there is a large LOCA and failure of the ECI system. The continuing research is focussed on fission-product chemistry (to establish what radioactive materials might become airborne) and hydrogen combustion (to establish the containment pressure and thus the potential leakage rate). These tasks are well advanced.

REFERENCES

1. F.W. Barclay, J.D. Bean and R.E. Nieman, "RAMA - A Computer Code for Prediction of Two-Phase Flow in Pipe Networks", presented at Intl. Assoc. of Science and Tech. for Development Symposium on Simulation, Modelling and Decision in Energy Systems, Montreal, 1978.

2. F.W. Barclay, R.E. Nieman and M.P. Hasinoff, "Transient Heat Transfer and Fluid Mechanics of a Recirculating Pressurized Water Loop During Blowdown and Cold Water Injection", Canadian Journal of Chemical Engineering 59, 201 (1981).

3. S. Banerjee and W.T. Hancox, "On the Development of Methods for Analysing Transient Flow-Boiling", Int. J. Multiphase Flow 4, 437 (1978).

4. S. Banerjee and A.M.C. Chan, "Separated Flow Models: Part I. Analysis of the Averaged and Local Instantaneous Formulations", Int. J. Multiphase Flow 6, 1 (1980).

5. W.T. Hancox, R.L. Ferch, W.S. Liu, and R.E. Nieman, "One-Dimensional Models for Transient Gas-Liquid Flows in Ducts", Int. J. Multiphase Flow 6, 25 (1980).

6. W.G. Mathers, W.W. Zuzak, B.H. McDonald and W.T. Hancox, "On Finite Difference Solutions to the Transient Flow-Boiling Equations", In Proceedings of the Committee for Safety of Nuclear Installations Specialists Meeting on Transient Two-Phase Flow, Toronto, 1976, Volume 1, p. 278. Atomic Energy of Canada Limited, Toronto, 1978.

7. W.T. Hancox and B.H. McDonald, "Finite Difference Algorithms to Solve the One-Dimensional Flow-Boiling Equations", In Proceedings of the ANS/AMSE/NRC International Topical Meeting on Nuclear Reactor Thermal-Hydraulics, Saratoga Springs, 1980. U.S. Nuclear Regulatory Commission Report, NUREG/CP-0014, Volume 2, p. 798.

8. D.J. Richards and B.H. McDonald, "A Dynamic Grid Point Allocation Scheme for the Characteristic Finite Difference Method", Atomic Energy of Canada Limited Report, AECL-7147 (1981).

9. W.T. Hancox and S. Banerjee, "Numerical Standards for Flow-Boiling Analysis", Nuc. Sci. and Eng. 64, 106 (1977).

10. R.L. Ferch, "Method of Characteristics Solutions for Non-Equilibrium Transient Flow-Boiling", Int. J. Multiphase Flow 5, 265 (1979).

11. S. Banerjee and W.T. Hancox, "Transient Thermohydraulics Analysis for Nuclear Reactors," Keynote Paper, In Proceedings of the Sixth International Heat Transfer Conference, Toronto, 1978, Volume 6, p. 311. Hemisphere, Washington, 1978.

12. S. Necmi and W.T. Hancox, "An Experimental and Theoretical Investigation of Blowdown from a Horizontal Pipe", In Proceedings of the Sixth International Heat Transfer Conference, Toronto, 1978, Volume 5, p. 83. Hemisphere, Washington, 1978.

13. V.S.V. Rajan, F.W. Barclay, E.H. Hawley, B.H. McDonald and B.N. Hanna, "RAMA: A Code for Analysis of the Thermalhydraulics of Horizontal Heated Channels in a Pipe Network", In Proceedings of the OECD/CSNI Specialists Meeting on Transient Two-Phase Flow, Pasadena, 1981. To be published.

14. V.S.V. Rajan and D.R.S. Daymond, unpublished work.

15. T.R. Heidrick, W.T. Hancox and D.M. Nguyen, "Centrifugal Pump Behaviour in Steady and Transient Steam-Water Flows", In Polyphase Flow in Turbomachinery, p. 139. American Society of Mechanical Engineers, 1978.

16. T.R. Heidrick, D.M. Nguyen and V.S.V. Rajan, "The Behaviour of Centrifugal Pumps in Steady and Transient Steam-Water Flows", In Proceedings of the ANS/ASME/NRC International Topical Meeting on Nuclear Reactor Thermal-hydraulics, Saratoga Springs, 1980. U.S. Nuclear Regulatory Commission Report, NUREG/CP-0014, Volume 1, p. 585.

17. C.G. Mewdell, W.C. Harrison, E.H. Hawley, R.S. Dumont and G.H. Green, "Development and Verification of a Space-Dependent Dynamic Model of a Natural Circulation Steam Generator", 2nd International Conference on Boiler Dynamics and Control in Nuclear Power Stations, Bournemouth, England, 1979 October.

18. N.L. Arrison, W.T. Hancox, M.T. Sulatisky and S. Banerjee, "Blowdown of a Recirculating Loop with Heat Addition", In Proceedings of the Conference on Heat and Fluid Flow in Water Reactor Safety, Institution of Mechanical Engineers, Manchester, 1977.

19. F.W. Barclay, E.H. Hawley and R.E. Nieman, "RD-12 Facility Description", Unpublished Whiteshell Nuclear Research Establishment Report, WNRE-496 (1980).

20. F.W. Barclay, T.E. MacDonald, D.J. Richards, H. Funasaka and M.P. Hasinoff, unpublished work.

21. F.W. Barclay, "Heated Blowdown Experiments carried out in the RD-12 Loop Using High Initial Temperature and Pressure", Unpublished Whiteshell Nuclear Research Establishment Report, WNRE-500 (1981).

22. H.E. Sills, "ELOCA: Fuel Element Behaviour During High-Temperature Transients", Atomic Energy of Canada Limited Report, AECL-6357 (1979).

23. H.E. Sills and R.A. Holt, "NIRVANA, A High-Temperature Creep Model for Zircaloy Fuel Sheathing", Atomic Energy of Canada Limited Report, AECL-6412 (1979).

24. H.E. Sills and R.A. Holt, "Predicting High-Temperature Transient Deformation from Microstructural Models", In ASTM Special Technical Publication 681, 1979, pp. 325-341.

25. S. Sagat, H.E. Sills and J.A. Walsworth, "Deformation and Failure of CANDU Fuel Sheaths Under LOCA Conditions", presented at the American Society for Testing and Materials Conference on Zirconium in the Nuclear Industry, Vancouver, 1982 June.

26. R.L. Varty and H.E. Rosinger, "A Failure Criterion Model for Thin-Walled Zircaloy-4 Tubes in the 900 to 1600 K Temperature Range", In Fracture Problems and Solutions in the Energy Industry, L.A. Simpson, Ed., Pergamon Press, Oxford, 1982 Spring.

27. A. Sawatzky, "A Proposed Criterion for the Oxygen Embrittlement of Zircaloy-4 Fuel Cladding", In ASTM Special Technical Publication 681, 1979, pp. 479-496.

28. A. Sawatzky, G.A. Ledoux and S. Jones, "Oxidation of Zirconium During a High Temperature Transient", In ASTM Special Technical Publication 633, 1977, pp. 134-149.

29. A. Wexler, G.I. Costache, G. Jeng, B. Fry and A. Sawatzky, "A Finite Element Computer Code for the Calculation of Oxygen Distribution Within Zirconium Alloy During a Temperature Transient," Atomic Energy of Canada Limited Report, in preparation.

30. S. Banerjee, J.H. Bridges, J.J.M. Too and T.R. Hsu, "A Model for Analysis of Fuel Behaviour in Transients", Nuc. Eng. Des. 42, 319 (1977).

31. J.J.M. Too and H. Tamm, "FAXMOL and its Application to the Prediction of High Temperature Creep and Sheath Ballooning Behaviour", Nuc. Eng. Des. 56, 211 (1980).

32. W.K. Snelson and M.F. Roett, unpublished data.

33. V.Q. Tang and D.G. Vandenberghe, "CHAN II: A Computer Program Predicting Fuel Channel Thermal Behaviour in a Typical CANDU-PHW Reactor Core Following a Loss-of-Coolant Accident", Unpublished Whiteshell Nuclear Research Establishment Report, WNRE-494 (1981).

34. V.F. Urbanic and T.R. Heidrick, "High Temperature Oxidation of Zircaloy-2 and Zircaloy-4 in Steam", J. Nuc. Mat. 75, 251 (1978).

35. Jules Thibault, "Boiling Heat Transfer Around a Horizontal Cylinder and in Tube Bundles", Ph.D. Thesis, McMaster University, 1978.

36. R.S.W. Shewfelt and J.D. Bean, unpublished work.

37. G.E. Gillespie, R.G. Moyer and R.S.W. Shewfelt, "Experiments to Investigate Moderator Boiling When a Pressure Tube Contacts its Calandria Tube", Unpublished Whiteshell Nuclear Research Establishment Report, WNRE-401 (1980).

38. G.E. Gillespie, "An Experimental Investigation of Heat Transfer from a Fuel Channel to Surrounding Water", In Proceedings of the Canadian Nuclear Society Conference, Ottawa, 1981, p. 157. Canadian Nuclear Society, Toronto.

39. R.J. Lemire, J. Paquette, D.F. Torgerson, D.J. Wren and J.W. Fletcher, Assessment of Iodine Behaviour in Reactor Containment Buildings from a Chemical Perspective", Atomic Energy of Canada Limited Report, AECL-6812 (1981).

40. D.F. Torgerson, R.J. Lemire, J. Paquette, D.J. Wren, and F. Garisto, "Iodine Source Term Under Reactor Accident Conditions", Atomic Energy of Canada Limited Report, AECL-7350 (1981).

41. D.D.S. Liu, R. MacFarlane and L.J. Clegg, "Ignition Behaviour of Hydrogen-Air Mixtures near Flammability Limits", paper presented to the Combustion Institute, Technical Meeting, Ottawa, 1981 May.

42. D.D.S. Liu, W.C. Harrison, H. Tamm, R. MacFarlane and L.J. Clegg, "Canadian Hydrogen Combustion Studies Related to Nuclear Reactor Safety Assessment", Atomic Energy of Canada Limited Report, AECL-6994 (1980).

43. S.R. Mulpuru and G.B. Wilkin, "A Model for Vented Deflagration of Hydrogen in a Volume", Atomic Energy of Canada Limited Report AECL-6826 (1982).

44. D.D.S. Liu, R. MacFarlane and L.J. Clegg, "Some Results of WNRE Experiments on Hydrogen Combustion", Atomic Energy of Canada Limited Report, AECL-7046 (1981).

45. H. Tamm, W.C. Harrison and R.K. Kumar, "Hydrogen Combustion Research at WNRE", to be published in Proceedings of the OECD/IGUS Specialists Meeting on Fuel-Air Explosions, Montreal, 1981 November.

ISSN 0067-0367

To identify individual documents in the series we have assigned an AECL- number to each.

Please refer to the AECL- number when requesting additional copies of this document from

Scientific Document Distribution Office
Atomic Energy of Canada Limited
Chalk River, Ontario, Canada
KOJ 1JO

Price: $4.00 per copy

ISSN 0067-0367

Pour identifier les rapports individuels faisant partie de cette série nous avons assigné un numéro AECL- à chacun.

Veuillez faire mention du numéro AECL -si vous demandez d'autres exemplaires de ce rapport au

Service de Distribution des Documents Officiels
L'Energie Atomique du Canada Limitée
Chalk River, Ontario, Canada
KOJ 1JO

prix: $4.00 par exemplaire